

# INDOLPhosphole and INDOLPhos Palladium–Allyl Complexes in Asymmetric Allylic Alkylations

Jeroen Wassenaar,<sup>†</sup> Steven van Zutphen,<sup>‡,§</sup> Guilhem Mora,<sup>‡</sup> Pascal Le Floch,<sup>‡</sup> Maxime A. Siegler,<sup>||</sup> Anthony L. Spek,<sup>||</sup> and Joost N. H. Reek<sup>\*,†</sup>

Van 't Hoff Institute for Molecular Sciences, University of Amsterdam, Nieuwe Achtergracht 166, 1018 WV Amsterdam, The Netherlands, Laboratoire "Hétéroéléments et Coordination", Ecole Polytechnique, CNRS, 91128 Palaiseau Cédex, France, and Crystal and Structural Chemistry, Bijvoet Centre for Biomolecular Research, Faculty of Science, Utrecht University, Padualaan 8, 3584 CH Utrecht, The Netherlands

Received December 19, 2008

The new INDOLPhosphole ligands **3a,b** are obtained in good yield in a two-step synthetic sequence from 3-methylindole, (*S*)-BINOL, and the corresponding cyanophosphole. Palladium–allyl complexes have been prepared from INDOLPhosphole (**3b**) and INDOLPhos (**1a**) of the type [Pd(INDOLPhos(*p*-hole))( $\eta^3$ -C<sub>3</sub>H<sub>5</sub>)]PF<sub>6</sub> and studied by multidimensional NMR spectroscopy and X-ray crystallography. The allyl ligand undergoes a  $\eta^3$ – $\eta^1$ – $\eta^3$  isomerization in these complexes, which is selective when **1a** is the ligand. A tetrameric, boxlike structure, encapsulating a PF<sub>6</sub><sup>−</sup> counteranion, is formed in the solid state in the case of complex **5** ([Pd(**3b**)( $\eta^3$ -C<sub>3</sub>H<sub>5</sub>)]PF<sub>6</sub>). INDOLPhosphole ligands **3a,b** and a small library of INDOLPhos ligands were screened in the Pd-catalyzed asymmetric allylic alkylation of mono- and disubstituted allylic acetates. The catalysts derived from these ligands were highly active, and enantioselectivities were obtained for 1,3-diphenylprop-2-enyl acetate up to 90% ee. Cinnamyl acetate was converted quantitatively with low regioselectivity (*b/l* = 14/86) and good enantioselectivity up to 81% ee. In the case of disubstituted substrates, the absolute configuration of the product could be rationalized by a model of selective attack on one of the enantiotopic termini in the Pd–allyl intermediate.

## Introduction

Chiral hybrid bidentate phosphine–phosphoramidite ligands have recently gained much attention from the synthetic community for their use in highly efficient asymmetric catalytic transformations.<sup>1</sup> Along with the renaissance of chiral monodentate ligands<sup>2</sup> and the introduction of supramolecular bidentate ligands,<sup>3</sup> hybrid ligands are among the most significant developments in the field of asymmetric transition-metal catalysis in the new millennium. In comparison to classical chiral bidentate phosphines such as BINAP and DuPHOS, hybrid ligands offer several advantages. First, the presence of two different phosphorus donor atoms, in addition to one or more chirality elements, results in desymmetrization of the coordination sphere

in the transition-metal complexes of hybrid ligands. This enables specific binding of prochiral substrates, thus providing an additional handle for enantiodiscrimination. Second, the facile preparation resulting from the often modular synthetic sequence in two or three steps allows for rapid scale-up for industrial use and provides an economical advantage over conventional chiral diphosphines.

In 2000, Leitner et al. introduced the first hybrid bidentate phosphine–phosphoramidite QUINAPHOS and demonstrated its use in the asymmetric Rh-catalyzed hydrogenation of dimethyl itaconate and methyl 2-acetamidoacrylate.<sup>4</sup> Up to now several other chiral phosphine–phosphoramidites have been

\* To whom correspondence should be addressed. E-mail: J.N.H.Reek@uva.nl. Fax: +31 (0)20 525 6422. Tel: +31 (0)20 525 6437.

<sup>†</sup> University of Amsterdam.

<sup>‡</sup> Ecole Polytechnique.

<sup>§</sup> Current address: Corning SAS, Corning European Technology Center, 77210 Avon, France.

<sup>||</sup> Utrecht University.

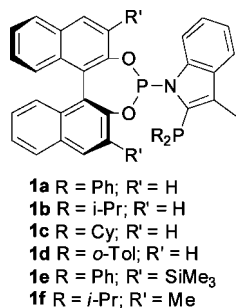
(1) (a) Amoroso, D.; Graham, T. W.; Guo, R. W.; Tsang, C. W.; Abdur-Rashid, K. *Aldrichim. Acta* **2008**, *41*, 15–26. (b) Boeda, F.; Beneyton, T.; Crévisy, C. *Mini-Rev. Org. Chem.* **2008**, *5*, 96–127.

(2) (a) Claver, C.; Fernandez, E.; Gillon, A.; Heslop, K.; Hyett, D. J.; Martorell, A.; Orpen, A. G.; Pringle, P. G. *Chem. Commun.* **2000**, 961–962. (b) Reetz, M. T.; Mehler, G. *Angew. Chem., Int. Ed.* **2000**, *39*, 3889. (c) van den Berg, M.; Minnaard, A. J.; Schudde, E. P.; van Esch, J.; de Vries, A. H. M.; de Vries, J. G.; Feringa, B. L. *J. Am. Chem. Soc.* **2000**, *122*, 11539–11540. (d) Minnaard, A. J.; Feringa, B. L.; Lefort, L.; De Vries, J. G. *Acc. Chem. Res.* **2007**, *40*, 1267–1277. (e) Norman, D. W.; Carraz, C. A.; Hyett, D. J.; Pringle, P. G.; Sweeney, J. B.; Orpen, A. G.; Phtemung, H.; Wingard, R. L. *J. Am. Chem. Soc.* **2008**, *130*, 6840–6847. (f) Reetz, M. T. *Angew. Chem., Int. Ed.* **2008**, *47*, 2556–2588. (g) Erre, G.; Enthaler, S.; Junge, K.; Gladiali, S.; Beller, M. *Coord. Chem. Rev.* **2008**, *252*, 471–491.

(3) (a) Slagt, V. F.; van Leeuwen, P. W. N. M.; Reek, J. N. H. *Chem. Commun.* **2003**, 2474–2475. (b) Takacs, J. M.; Reddy, D. S.; Moteki, S. A.; Wu, D.; Palencia, H. *J. Am. Chem. Soc.* **2004**, *126*, 4494–4495. (c) Breit, B. *Angew. Chem., Int. Ed.* **2005**, *44*, 6816–6825. (d) Kleij, A. W.; Reek, J. N. H. *Chem. Eur. J.* **2006**, *12*, 4219–4227. (e) Kuil, M.; Goudriaan, P. E.; van Leeuwen, P. W. N. M.; Reek, J. N. H. *Chem. Commun.* **2006**, 4679–4681. (f) Sandee, A. J.; Reek, J. N. H. *Dalton Trans.* **2006**, 3385–3391. (g) Flapper, J.; Reek, J. N. H. *Angew. Chem., Int. Ed.* **2007**, *46*, 8590–8592. (h) Kuil, M.; Goudriaan, P. E.; Kleij, A. W.; Tooke, D. M.; Spek, A. L.; van Leeuwen, P. W. N. M.; Reek, J. N. H. *Dalton Trans.* **2007**, 2311–2320. (i) Sandee, A. J.; van der Burg, A. M.; Reek, J. N. H. *Chem. Commun.* **2007**, 864–866. (j) Goudriaan, P. E.; van Leeuwen, P. W. N. M.; Birkholz, M. N.; Reek, J. N. H. *Eur. J. Inorg. Chem.* **2008**, 2939–2958. (k) Laungani, A. C.; Slattery, J. M.; Krossing, I.; Breit, B. *Chem. Eur. J.* **2008**, *14*, 4488–4502. (l) Moteki, S. A.; Takacs, J. M. *Angew. Chem., Int. Ed.* **2008**, *47*, 894–897. (m) Patureau, F. W.; Kuil, M.; Sandee, A. J.; Reek, J. N. H. *Angew. Chem., Int. Ed.* **2008**, *47*, 3180–3183.

(4) (a) Francio, G.; Faraone, F.; Leitner, W. *Angew. Chem., Int. Ed.* **2000**, *39*, 1428. (b) Burk, S.; Francio, G.; Leitner, W. *Chem. Commun.* **2005**, 3460–3462. (c) Diez-Holz, C. J.; Boing, C.; Francio, G.; Holscher, M.; Leitner, W. *Eur. J. Org. Chem.* **2007**, 2995–3002.

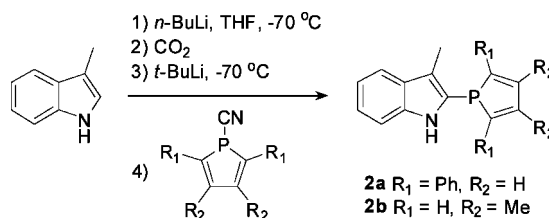
Chart 1. Structure of INDOLPhos Ligands 1a–f



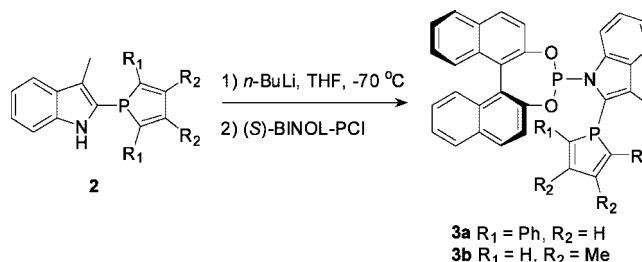
reported, such as ferrocene-based derivatives,<sup>5</sup> PEAPhos,<sup>6</sup> NOBIN-based derivatives,<sup>7</sup> Me-AnilaPhos,<sup>8</sup>  $\beta$ -amino alcohol based derivatives,<sup>9</sup> THNA-Phos,<sup>10</sup> and HY-Phos.<sup>11</sup> The ligands have been employed in a range of asymmetric transformations, including Rh- and Ru-catalyzed hydrogenation, hydroformylation, and Cu-catalyzed conjugate addition to enones. Our group contributed to this field with the development of INDOLPhos (**1**), which is based on a rigid 3-methylindole backbone, resulting in a very small bite angle (Chart 1).<sup>12</sup> Good to excellent enantioselectivities were obtained using this ligand in Rh-catalyzed hydrogenation and hydroformylation. It was observed that the steric and electronic properties of the phosphine part played a crucial role in obtaining high selectivities in these transformations. Changing a diphenylphosphine for a diisopropylphosphine results in some cases in an increase of enantioselectivity up to 90% ee. Encouraged by these findings, we aimed to introduce more variation on this position. Phospholes, unsaturated phosphorus-containing five-membered heterocycles, exhibit steric and electronic properties different from those of phosphines, making them suitable candidates to introduce more variety on the INDOLPhos platform.<sup>13</sup>

Phosphole derivatives were found to show excellent activity in Pd-catalyzed allylic substitution, prompting us to investigate the reactivity of the phosphole-containing INDOLPhos derivatives in this transformation.<sup>14</sup> To the best of our knowledge, hybrid phosphine–phosphoramidite ligands have not been

Scheme 1. Synthesis of Indolyphospholes 2a,b



Scheme 2. Synthesis of INDOLPhospholes 3a,b



used up to now in this reaction, despite their potential for direct nucleophilic attack specifically at one position of the coordinated allyl.<sup>15,16</sup> However, excellent results in asymmetric allylic alkylation have been obtained with diphosphites and phosphite–phosphoramidites.<sup>17</sup> Here, we introduce INDOLPhospholes as a new class of hybrid phosphole–phosphoramidite ligands and describe their synthesis, coordination properties, and reactivity in Pd-catalyzed asymmetric allylic alkylation. Furthermore, INDOLPhos palladium complexes are described along with their catalytic performance in the asymmetric allylic alkylation.

## Results and Discussion

**Ligand Synthesis.** INDOLPhosphole ligands **3** were prepared in a two-step procedure analogous to the synthesis of INDOLPhos ligands **1**.<sup>12</sup> Instead of reacting 3-methylindole with a chlorophosphine, *P*-cyano 2,5-diphenyl (DPP) and 3,4-dimethyl (DMP) phospholes were used as electrophiles. The cyanophospholes were selected instead of their chloro and bromo derivatives, which are very reactive and difficult to handle.<sup>18</sup> In the first step, the 3-methylindole NH is in situ protected with carbon dioxide, which also acts as a directing group for the selective deprotonation at the 2-position of the indole (Scheme 1). Addition of the corresponding cyanophosphole gives indolyphospholes **2a,b** as yellow and white solids, respectively, in moderate to good yields (71–84%), requiring no chromatographic workup. Deprotonation of the NH of the indolyphospholes **2** at low temperature followed by condensation with (*S*)-binaphthol phosphorochloridite results in the formation of INDOLPhosphole ligands **3a,b** (Scheme 2). They are obtained in moderate yield (48–63%) after chromatographic purification as yellow and white solids, respectively.

(15) For reviews on Pd-catalyzed allylic alkylation, see: (a) Trost, B. M.; Van Vranken, D. L. *Chem. Rev.* **1996**, *96*, 395–422. (b) Trost, B. M.; Crawley, M. L. *Chem. Rev.* **2003**, *103*, 2921–2943.

(16) Evans, L. A.; Fey, N.; Harvey, J. N.; Hose, D.; Lloyd-Jones, G. C.; Murray, P.; Orpen, A. G.; Osborne, R.; Owen-Smith, G. J. J.; Purdie, M. J. *Am. Chem. Soc.* **2008**, *130*, 14471–14473.

(17) (a) Diéguez, M.; Pàmies, O.; Claver, C. *J. Org. Chem.* **2005**, *70*, 3363–3368. (b) Mata, Y.; Claver, C.; Diéguez, M.; Pàmies, O. *Tetrahedron: Asymmetry* **2006**, *17*, 3282–3287. (c) Pàmies, O.; Diéguez, M.; Claver, C. *Adv. Synth. Catal.* **2007**, *349*, 836–840. (d) den Heeten, R.; Swennenhuis, B. H. G.; van Leeuwen, P. W. N. M.; de Vries, J. G.; Kamer, P. C. *Angew. Chem., Int. Ed.* **2008**, *47*, 6602–6605.

(18) Charrier, C.; Bonnard, H.; Mathey, F.; Neibecker, D. *J. Organomet. Chem.* **1982**, *231*, 361–367.

(5) (a) Hu, X. P.; Zheng, Z. *Org. Lett.* **2004**, *6*, 3585–3588. (b) Jia, M.; Li, X. S.; Lam, W. S.; Kok, S. H. L.; Xu, L. J.; Lu, G.; Yeung, C. H.; Chan, A. S. C. *Tetrahedron: Asymmetry* **2004**, *15*, 2273–2278. (c) Hu, X. P.; Zhuo, Z. *Org. Lett.* **2005**, *7*, 419–422. (d) Zeng, Q. H.; Hu, X. P.; Duan, Z. C.; Liang, X. M.; Zheng, Z. *Tetrahedron: Asymmetry* **2005**, *16*, 1233–1238.

(6) Huang, J. D.; Hu, X. P.; Duan, Z. C.; Zeng, Q. H.; Yu, S. B.; Deng, J.; Wang, D. Y.; Zheng, Z. *Org. Lett.* **2006**, *8*, 4367–4370.

(7) Yan, Y. J.; Zhang, X. M. *J. Am. Chem. Soc.* **2006**, *128*, 7198–7202.

(8) Vallianatou, K. A.; Kostas, I. D.; Holz, J.; Börner, A. *Tetrahedron Lett.* **2006**, *47*, 7947–7950.

(9) Boeda, F.; Rix, D.; Clavier, H.; Crévisy, C.; Mauduit, M. *Tetrahedron: Asymmetry* **2006**, *17*, 2726–2729.

(10) (a) Wang, D. Y.; Hu, X. P.; Huang, J. D.; Deng, J.; Yu, S. B.; Duan, Z. C.; Xu, X. F.; Zheng, Z. *Angew. Chem., Int. Ed.* **2007**, *46*, 7810–7813. (b) Qiu, M.; Hu, X. P.; Wang, D. Y.; Deng, J.; Huang, J. D.; Yu, S. B.; Duan, Z. C.; Zheng, Z. *Adv. Synth. Catal.* **2008**, *350*, 1413–1418.

(11) Yu, S.-B.; Huang, J.-D.; Wang, D.-Y.; Hu, X.-P.; Deng, J.; Duan, Z.-C.; Zheng, Z. *Tetrahedron: Asymmetry* **2008**, *19*, 1862.

(12) (a) Wassenaar, J.; Reek, J. N. H. *Dalton Trans.* **2007**, 3750–3753. (b) Wassenaar, J.; Kuil, M.; Reek, J. N. H. *Adv. Synth. Catal.* **2008**, *350*, 1610–1614.

(13) (a) Mathey, F. In *Phosphorus-Carbon Heterocyclic Chemistry: The Rise of a New Domain*; Mathey, F., Ed.; Pergamon: Amsterdam, 2001; p 753. (b) Quin, L. D. In *Phosphorus-Carbon Heterocyclic Chemistry: The Rise of a New Domain*; Mathey, F., Ed.; Pergamon: Amsterdam, 2001; p 219.

(14) (a) Thoumasset, C.; Grutzmacher, H.; Deschamps, B.; Ricard, L.; Le Floch, P. *Eur. J. Inorg. Chem.* **2006**, 3911–3922. (b) Mora, G.; Deschamps, B.; van Zutphen, S.; Le Goff, X. F.; Ricard, L.; Le Floch, P. *Organometallics* **2007**, *26*, 1846–1855.

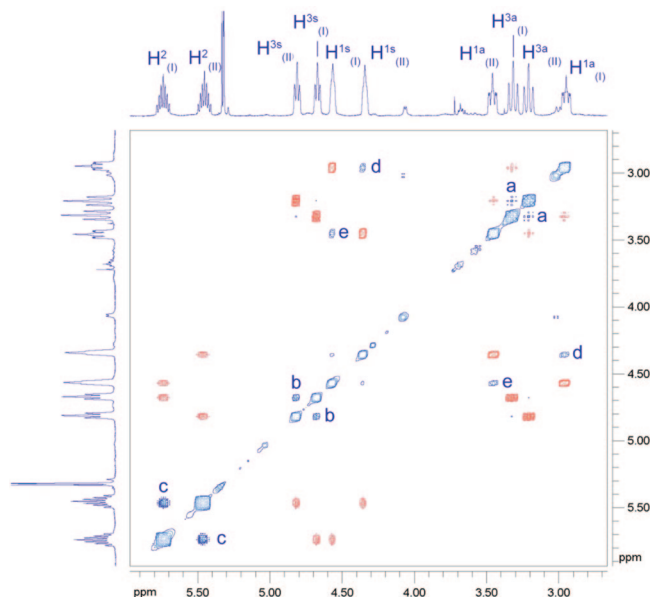


**Figure 1.** Section of the phase-sensitive  $^1\text{H}$  2D NOESY spectrum ( $\text{CD}_2\text{Cl}_2$ , 500 MHz, 298 K) for complex **4a**. The blue off-diagonal peaks arise from exchange, whereas the red peaks arise from NOE.

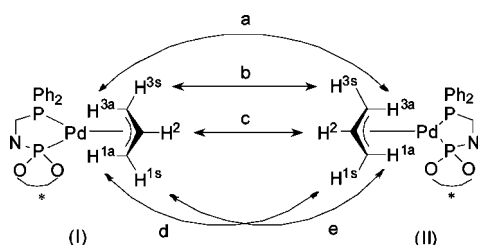
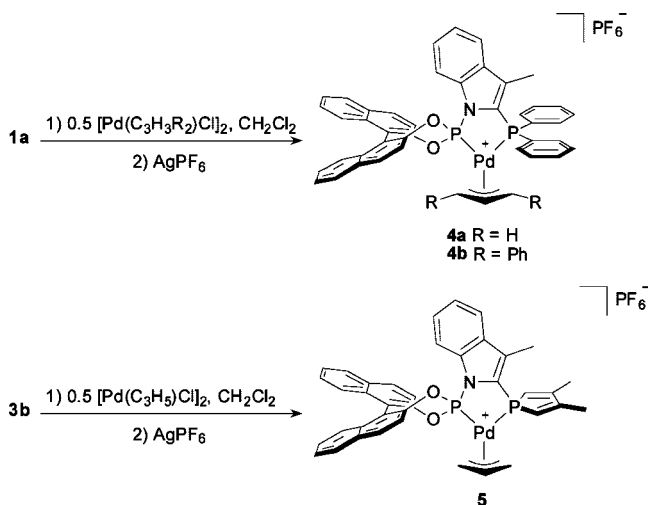
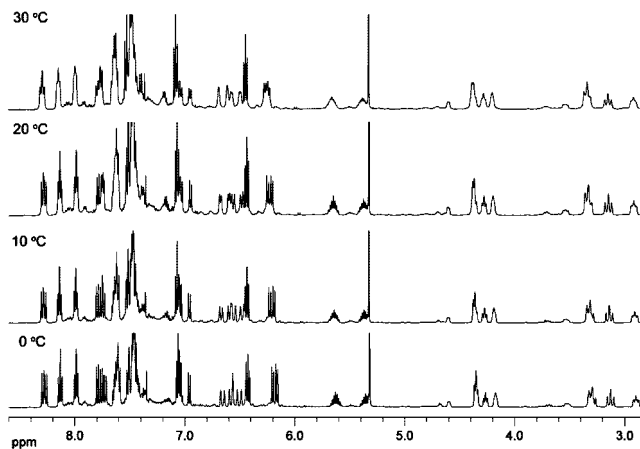


**Figure 2.** Exchange pathways interconverting isomers I and II of complex **4a**.

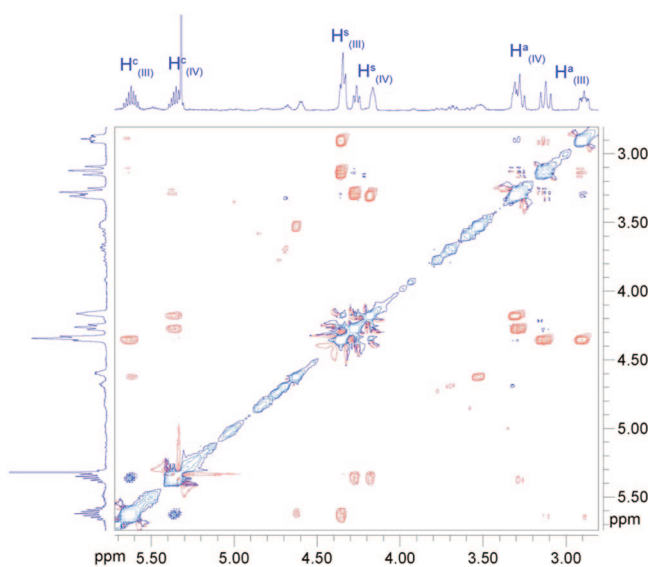
### Scheme 3. Synthesis of Palladium–Allyl Complexes **4** and **5**



We reported previously that the  $^{31}\text{P}$  NMR signals of INDOL-Phos ligands **1** exhibit large coupling constants in the range of 200 Hz.<sup>12a</sup> Their phosphole derivatives **3**, on the other hand, do not exhibit such large couplings, but the  $^{31}\text{P}$  NMR spectrum of **3a** exhibits two singlets. Two doublets are obtained for **3b** with a coupling constant of 43.1 Hz. The large difference in these parameters can be attributed to the difference in electronic properties of phospholes compared to phosphines.



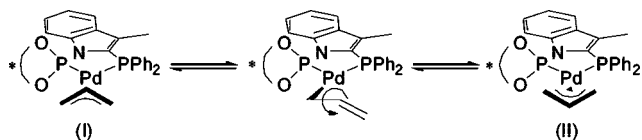
**Figure 3.**  $^1\text{H}$  VT NMR spectra ( $\text{CD}_2\text{Cl}_2$ , 500 MHz) of complex **5**.



**Figure 4.** Section of the phase-sensitive  $^1\text{H}$  2D NOESY spectrum ( $\text{CD}_2\text{Cl}_2$ , 500 MHz, 263 K) for complex **5**. The blue off-diagonal peaks arise from exchange, whereas the red peaks arise from NOE.

**Synthesis of Palladium–Allyl Complexes.** The coordination properties of ligands **1a** and **3b** were investigated in their cationic palladium–allyl complexes. Reaction of the ligand with 0.5 equiv of  $[\text{Pd}_2(\eta^3\text{-C}_3\text{H}_5)_2\text{Cl}_2]$  in dichloromethane followed by abstraction of the chloride with  $\text{AgPF}_6$  afforded **4a** and **5** as pale yellow solids in good to excellent yield (79–99%, Scheme 3). Similarly, the bright yellow Pd–diphenylallyl complex **4b** was obtained in 60% yield using  $[\text{Pd}_2(\eta^3\text{-1,3-diphenylallyl})_2\text{Cl}_2]$  and **1a**. The allyl complexes have been fully characterized by NMR techniques ( $^1\text{H}$ ,  $^{31}\text{P}$ ,  $^{13}\text{C}$ ), mass spectrometry, and X-ray crystallography. Phosphole **3a** was also reacted with the Pd–allyl chloride dimer, resulting in the formation of the desired coordination compound in a complex product matrix from which isolation proved impossible.

**NMR Study of Palladium–Allyl Complexes.** Complexes **4a,b** and **5** were studied by one- and two-dimensional NMR in order to determine their structure in solution. Complex **4a** displays duplicated signals for all allyl protons and for some of the protons on the INDOLPhos ligand. This effect can be attributed to isomerism of the allyl fragment, which can adopt two orientations (Figure 2). The isomers are able to interconvert

Scheme 4. Mechanism of  $\eta^3$ – $\eta^1$ – $\eta^3$  Isomerization in Complex 4aTable 1. Thermodynamic Parameters for the  $\eta^3$ – $\eta^1$ – $\eta^3$  Isomerization in Complex 5

param	value
$E_a^a$ (kcal mol <sup>-1</sup> )	21.0
$\Delta G^{\ddagger a}$ (kcal mol <sup>-1</sup> )	16.3
$\Delta H^{\ddagger}$ (kcal mol <sup>-1</sup> )	20.4
$\Delta S^{\ddagger}$ (kcal mol <sup>-1</sup> K <sup>-1</sup> )	$1.4 \times 10^{-2}$
$k^b$ (s <sup>-1</sup> )	3.6

<sup>a</sup> At 298 K. <sup>b</sup> Rate of exchange at 293 K.

via a formal  $\pi$ -rotation involving a  $\eta^3$ – $\eta^1$ – $\eta^3$  isomerization. It was found previously in JOSIPHOS<sup>19</sup> and other bidentate ligands containing different phosphorus donor atoms<sup>20</sup> that this isomerization is selective, involving opening of only one Pd–C bond of the allyl fragment. In order to establish if such a selectivity is also present in complex **4a**, a phase-sensitive <sup>1</sup>H 2D NOESY experiment was carried out (Figure 1). The spectrum shows exchange peaks (blue) for the central proton H<sup>2</sup> of both isomers and their selective NOE contacts (red) with the syn protons within each isomer. There is no exchange of syn and anti protons at C<sub>3</sub>; i.e., H<sup>3s</sup> of isomer I becomes H<sup>3s</sup> of isomer II and likewise for H<sup>3a</sup>. At C<sub>1</sub>, on the other hand, syn–anti exchange does occur, interconverting H<sup>1s</sup> of isomer I into H<sup>1a</sup> of isomer II and vice versa. The exchange pathways are summarized in Figure 2.

The selective syn–anti exchange at C<sub>1</sub>, cis to the phosphoramidite moiety, indicates that the  $\eta^3$ – $\eta^1$ – $\eta^3$  isomerization follows a mechanism in which the Pd–C<sub>3</sub> bond opens, forming a  $\eta^1$  transition state wherein the C<sub>1</sub>–C<sub>2</sub> bond rotates 180°, completed by re-formation of the  $\eta^3$ -allyl (Scheme 4). Importantly, the selective opening of the  $\eta^3$ -allyl occurs cis to the phosphine and can be rationalized by the greater steric bulk of the diphenylphosphine, as was observed earlier in related systems.<sup>19b</sup> The increased Pd–C<sub>3</sub> bond length in the crystal structure of **4a** supports this observation (vide infra).

The room-temperature <sup>1</sup>H NMR spectrum of complex **5** exhibits broad signals for all protons except for the indole backbone protons. A variable-temperature NMR study was performed to analyze the dynamic process (Figure 3). The broadening can be attributed to a faster  $\eta^3$ – $\eta^1$ – $\eta^3$  isomerization compared to that for complex **4a**, as individual signals are obtained for the allyl protons of both isomeric complexes III and IV. The coalescence temperature could unfortunately not be established in CD<sub>2</sub>Cl<sub>2</sub>, the only suitable solvent with regard to stability and solubility of the complex, due to its low boiling point. Nevertheless, using line shape analysis at various temperatures, the thermodynamic parameters for the isomerization could be determined (Table 1). The free energy of activation is found to be 16.3 kcal mol<sup>-1</sup>, which is in good agreement with previous measurements of dynamic palladium–allyl complexes.<sup>21</sup> The positive entropy contribution results from the additional degree of freedom gained from the intramolecular

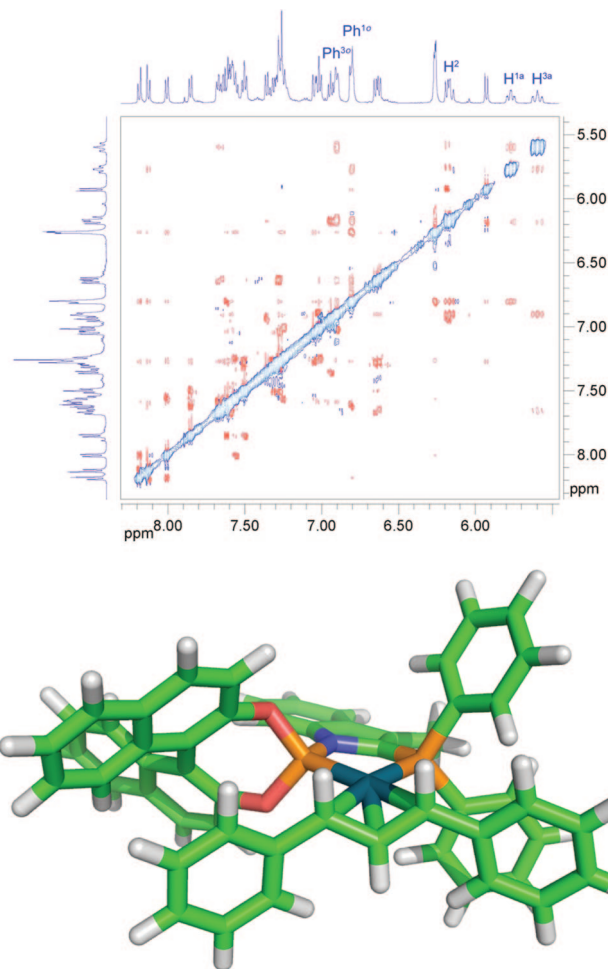


**Figure 5.** (top) Section of the phase-sensitive <sup>1</sup>H 2D NOESY spectrum (CDCl<sub>3</sub>, 500 MHz, 298 K) for complex **5**. The blue off-diagonal peaks arise from exchange, whereas the red peaks arise from NOE. (bottom) Calculated lowest energy structure of **4b** (DFT, BP86, SV(P)): green for C, blue for N, red for O, orange for P, aquamarine for Pd.

isomerization. At 20 °C, the rate of exchange is 3.6 s<sup>-1</sup>. However, this rate cannot be related to the catalytic experiments, as substituted allyl ligands are known to isomerize much more slowly, if at all.<sup>15a</sup>

The <sup>1</sup>H 2D NOESY spectrum of complex **5** was recorded at –10 °C (Figure 4). As for complex **4a**, the central allyl protons are exchanged in the  $\eta^3$ – $\eta^1$ – $\eta^3$  isomerization. All syn and anti allyl protons of one isomer exhibit exchange peaks with the signals for the other rotational isomer, although with low intensity. This implies that the isomerization is unselective, and Pd–C bond opening occurs at both termini of the allyl ligand. The decreased steric demand of the 3,5-dimethylphosphole in **5** compared to the diphenylphosphine in **4a** leads both donor atoms (phosphoramidite and phosphole) to be similar in size and, thus, no selective bond opening occurs.

The phenyl allyl complex **4b** does not exhibit rotational isomerism in solution or syn–anti interconversion. The <sup>1</sup>H 2D NOESY spectrum shows no off-diagonal exchange signals but only signals arising from NOE (Figure 5). In spite of the severe overlap of signals, the signals stemming from the phenylallyl fragment could be assigned unambiguously. NOE contacts

(19) (a) Breutel, C.; Pregosin, P. S.; Salzmann, R.; Togni, A. *J. Am. Chem. Soc.* **1994**, *116*, 4067–4068. (b) Pregosin, P. S.; Salzmann, R.; Togni, A. *Organometallics* **1995**, *14*, 842–847.

(20) Camus, J. M.; Andrieu, J.; Richard, P.; Poli, R. *Eur. J. Inorg. Chem.* **2004**, 1081–1091.

(21) Fernández-Galán, R.; Jalón, F. A.; Manzano, B. R.; Rodríguez de la Fuente, J.; Vrahami, M.; Jedlicka, B.; Weissensteiner, W.; Jögl, G. *Organometallics* **1997**, *16*, 3758–3768.

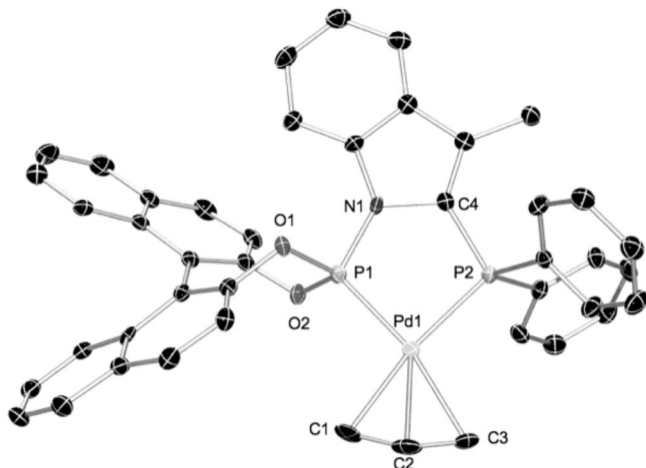


**Figure 6.** Displacement ellipsoid plot (50% probability level) of one Pd complex of **4a**. Hydrogen atoms are omitted for clarity. Selected bond distances (Å) and angles (deg): C(1)–C(2), 1.393(9); C(2)–C(3), 1.373(11); Pd(1)–C(1), 2.167(12); Pd(1)–C(2), 2.183(4); Pd(1)–C(3), 2.218(15); Pd(1)–P(1), 2.2255(7); Pd(1)–P(2), 2.2844(7); P(1)–N(1), 1.688(2); P(2)–C(4), 1.812(3); C(2)–Pd(1)–P(1), 134.15(13); C(2)–Pd(1)–P(2), 135.80(13); P(1)–Pd(1)–P(2), 87.93(3).

between one of the anti allyl protons ( $H^{1a}$ ) and the adjacent phenyl ring with the downfield bisnaphthol protons (top left of the NOESY spectrum) indicate that the phenyl group of the allyl fragment points away from the bulk imposed by the chiral bisnaphthol moiety. The contacts are confirmed by the DFT calculated structure (BP86, SV(P)) shown in Figure 5, which lies 0.5 kcal mol<sup>-1</sup> lower in energy than the other possible rotational isomer. According to the Boltzmann distribution, this other isomer is accessible and, indeed, the <sup>31</sup>P NMR spectrum shows the presence of a second species in trace amounts (<2%), which may be assigned to the second rotational isomer. As **4b** is the key catalytic intermediate in the allylic alkylation of *rac*-1,3-diphenylprop-2-enyl acetate, nucleophilic attack at this species leads to the product and determines the enantioselectivity (vide infra).

**X-ray Crystallography.** Crystals of complexes **4a** and **5** suitable for single-crystal X-ray diffraction were obtained by slow diffusion of hexanes into a saturated dichloromethane solution. Displacement ellipsoid plots for compounds **4a** and **5** are shown in Figures 6 and 7, respectively. The relevant bond distances and angles are listed in the corresponding figure captions.

In the crystal structure of **5**, the four crystallographically independent Pd complexes and two of the four independent PF<sub>6</sub><sup>-</sup> counteranions of the asymmetric unit form two-dimensional (hereafter, 2-D) planes parallel to (001). Along these planes, each PF<sub>6</sub><sup>-</sup> counterion is encapsulated into a tetrameric box built of the four independent cations (Figure 8). The formation of these tetrameric boxes can be attributed to weak C–H···F intermolecular interactions (C···F distances (C = carbon atoms of the allyl groups/phosphole rings/bisnaphthol moieties) vary in the range 3.23–3.54 Å; all standard uncertainties are lower than 0.01 Å) and the templating effect of the two spherical PF<sub>6</sub><sup>-</sup> counteranions. Within each tetrameric box, the four independent Pd complexes are always found in close contacts with each other. These contacts are found between (i) one proton of the bisnaphthol moiety of one complex and the  $\pi$ -system of the bisnaphthol moiety of the adjacent complex, (ii) one indole proton of one complex and the  $\pi$ -system of the bisnaphthol moiety of the adjacent complex, and (iii) one proton

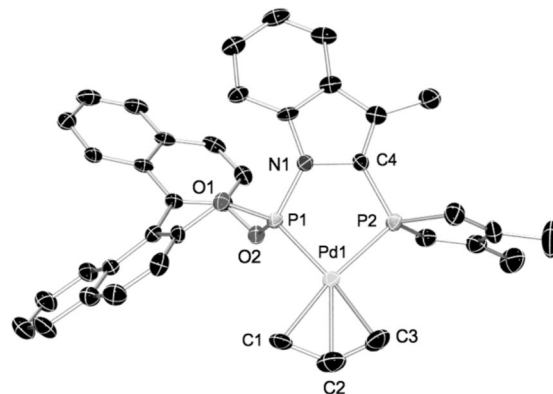


**Figure 7.** Displacement ellipsoid plot (50% probability level) of one Pd complex of **5**. Hydrogen atoms are omitted for clarity. Selected bond distances (Å) and angles (deg): C(1)–C(2), 1.382(6); C(2)–C(3), 1.357(6); Pd(1)–C(1), 2.170(3); Pd(1)–C(2), 2.157(4); Pd(1)–C(3), 2.181 (4); Pd(1)–P(1), 2.2243(8); Pd(1)–P(2), 2.2870(9); P(1)–N(1), 1.680(3); P(2)–C(4), 1.794(3); C(2)–Pd(1)–P(1), 138.34(13); C(2)–Pd(1)–P(2), 134.20(13); P(1)–Pd(1)–P(2), 85.80(3).

of the allyl ligand of one complex and the  $\pi$ -system of the indole moiety of the adjacent complex. There is no evidence that the tetrameric boxes are stable in solution. The presence of the phosphole ligand might be important for the formation of the box structure, which is not found in the crystal structure of **4a**.

The remaining independent PF<sub>6</sub><sup>-</sup> counteranions and lattice solvent molecules (i.e., dichloromethane) are found to be intercalated between the 2-D planes including the tetrameric boxes. These counteranions are in short contact with the Pd complexes via C–H···F interactions, which are comparable with those found for other encapsulated anions.<sup>22</sup>

The structures of **4a** and **5** both display a square-planar geometry around the palladium atom. Differences in the structures mainly arise from the increased bulkiness of the diphenylphosphine compared to the phosphole. This is reflected in the larger bite angle and Pd(1)–C(3) distance for **4a**. In addition, the phosphoramidite group in **5** is tilted out of the coordination plane, which is probably the result of packing effects which allow for the formation of the tetrameric box.

**Palladium-Catalyzed Asymmetric Allylic Alkylation.** The catalytic activity of the Pd complexes of ligands **1a–f** and **3a,b** was evaluated in the palladium-catalyzed asymmetric allylic substitution. Preliminary experiments using nitrogen nucleophiles in this reaction such as aniline and benzylamine did not yield the desired products. Therefore, dimethyl malonate was chosen as the nucleophile in the alkylation of racemic allylic acetates. Catalysts were generated in situ from [Pd<sub>2</sub>( $\eta^3$ -C<sub>3</sub>H<sub>5</sub>)<sub>2</sub>Cl<sub>2</sub>] and the corresponding ligand.

All ligands provided active catalysts for the allylic alkylation of *rac*-1,3-diphenylprop-2-enyl acetate **6**, a benchmark substrate for new ligands in the asymmetric allylic alkylation (Table 2). The reactivity and selectivity are highly affected by the ligand substituents and nature of the phosphine donor group. For INDOLPhos ligands **1a–d**, which vary only in the type of phosphine, similar reactivities are observed (entries 1–4). Sterically more demanding phosphines give rise to higher *ee*'s compared to diphenylphosphine, whereas the electronic properties seem to be less important. When substituents are introduced

(22) Li, C.; Pattacini, R.; Graff, R.; Braunstein, P. *Angew. Chem., Int. Ed.* **2008**, *47*, 6856–6859.

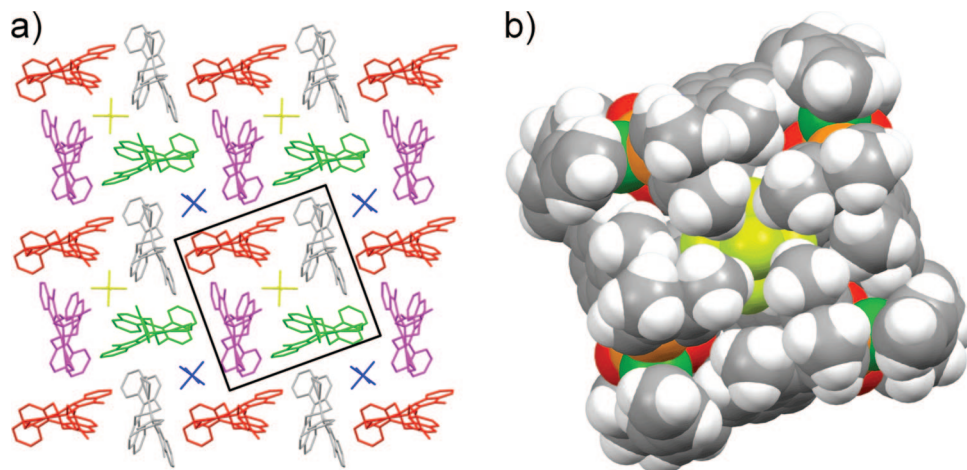


**Figure 8.** (a) Packing of one 2-D plane built of the four independent Pd complexes and two of the four independent  $\text{PF}_6^-$  counteranions, the view being down the normal to (001) in the crystal structure of **5**. The symmetry-independent residues are rendered in different colors. The black outline corresponds to one tetrameric box. The disorder of one allyl ligand and of one  $\text{PF}_6^-$  counteranion and the H atoms are omitted for the sake of clarity. (b) One tetrameric box in space-filling style (gray for C, blue for N, red for O, orange for P, yellow for F, green for Pd) projected down the  $c^*$  direction. The disorder of one allyl ligand is omitted for clarity.

**Table 2.** Pd-Catalyzed Allylic Alkylation of **6** with Ligands **1** and **3**<sup>a</sup>

entry	ligand	conv. (%) <sup>b</sup>	ee (%) <sup>c</sup>
1	<b>1a</b> (R = Ph, R' = H)	100	43
2	<b>1b</b> (R = <i>i</i> -Pr, R' = H)	100	70
3	<b>1c</b> (R = Cy, R' = H)	90	64
4	<b>1d</b> (R = <i>o</i> -Tol, R' = H)	100	66
5	<b>1e</b> (R = Ph, R' = SiMe <sub>3</sub> )	15	90
6	<b>1f</b> (R = <i>i</i> -Pr, R' = Me)	18	74
7	<b>3a</b> (R <sup>1</sup> = Ph, R <sup>2</sup> = H)	99	32
8	<b>3b</b> (R <sup>1</sup> = H, R <sup>2</sup> = Me)	100	56

<sup>a</sup> Conditions: 0.5 mol % of  $[\text{Pd}_2(\eta^3\text{-C}_3\text{H}_5)_2\text{Cl}_2]$ , 1.1 mol % of ligand,  $\text{CH}_2\text{Cl}_2$ , room temperature, 3 equiv of dimethyl malonate, 3 equiv of BSA, pinch of KOAc. <sup>b</sup> Conversion percentage of acetate after 1 h, determined by GC. <sup>c</sup> Enantiomeric excess, determined by chiral HPLC (Chiralcel-ODH). The *S* enantiomer was obtained in all cases.

at the 3- and 3'-positions on the binaphthol moiety, the reactivity decreases, whereas the ee increases up to 90% (entries 5 and 6).

INDOLPhospholes **3a,b** both give full conversion and enantioselectivities of 32% and 56%, respectively (entries 7 and 8). Surprisingly, the sterically less congested phosphole now gives higher selectivity, which is in contrast with the trend observed for INDOLPhos ligands **1a–d** as discussed above.

From the screening experiments outlined above, it was observed that ligand **1e** gave rise to the highest enantioselectivity but showed only 15% conversion after 1 h of reaction. However, longer reaction times allow for quantitative formation of the product. A solvent study using **1e** as ligand was carried out, with the aim of increasing activity while maintaining the high selectivity (Table 3). Acetonitrile proves to be the only solvent, giving a significantly higher rate compared to dichloromethane (entry 3). However, the enantioselectivity drops to 76% ee. The tradeoff in selectivity is not compensated by the gain in activity, and we thus carried out all further experiments using dichloromethane as solvent.

To investigate the effect of the structure of the substrate on the catalytic performance, *rac*-1,3-dimethylprop-2-enyl acetate (**8**) was subjected to the alkylation conditions (Table 4). It is known that exchanging the Ph group for a Me group results in

**Table 3.** Pd-Catalyzed Allylic Alkylation of **6** with Ligand **1e**<sup>a</sup>

entry	solvent	conv. (%) (time (h)) <sup>b</sup>	ee (%) <sup>c</sup>
1	$\text{CH}_2\text{Cl}_2$	100 (8)	90
2	THF	84 (4)	70
3	MeCN	100 (1)	76
4	EtOAc	65 (4)	68
5	toluene	74 (4)	85
6	<i>i</i> -PrOH	0 (22)	

<sup>a</sup> Conditions: 0.5 mol % of  $[\text{Pd}_2(\eta^3\text{-C}_3\text{H}_5)_2\text{Cl}_2]$ , 1.1 mol % of **1e**, room temperature, 3 equiv of dimethyl malonate, 3 equiv of BSA, pinch of KOAc. <sup>b</sup> Conversion percentage of acetate, determined by GC. The reaction time in hours is shown in parentheses. <sup>c</sup> Enantiomeric excess, determined by chiral HPLC (Chiralcel-ODH).

**Table 4.** Pd-Catalyzed Allylic Alkylation of **8** with Ligands **1** and **3**<sup>a</sup>

entry	ligand	conv. (%) <sup>b</sup>	ee (%) <sup>c</sup>
1	<b>1a</b> (R = Ph, R' = H)	100	31
2	<b>1b</b> (R = <i>i</i> -Pr, R' = H)	100	21
3	<b>1c</b> (R = Cy, R' = H)	100	20
4	<b>1d</b> (R = <i>o</i> -Tol, R' = H)	100	51
5	<b>1e</b> (R = Ph, R' = SiMe <sub>3</sub> )	100	39
6	<b>1f</b> (R = <i>i</i> -Pr, R' = Me)	100	15
7	<b>3a</b> (R <sup>1</sup> = Ph, R <sup>2</sup> = H)	57	35
8	<b>3b</b> (R <sup>1</sup> = H, R <sup>2</sup> = Me)	100	26

<sup>a</sup> Conditions: 0.5 mol % of  $[\text{Pd}_2(\eta^3\text{-C}_3\text{H}_5)_2\text{Cl}_2]$ , 1.1 mol % of ligand,  $\text{CH}_2\text{Cl}_2$ , room temperature, 3 equiv of dimethyl malonate, 3 equiv of BSA, pinch of KOAc. <sup>b</sup> Conversion percentage of acetate after 1 h, determined by GC. <sup>c</sup> Enantiomeric excess, determined by chiral GC (Chiralcel DEX CB).

most cases in lower enantioselectivity and rate enhancement.<sup>15a</sup> This is also observed for the catalysts generated from ligands **1** and **3**. Remarkably, the enantioselectivities obtained with arylphosphine-substituted ligands are lowered to a lesser extent than with alkylphosphines (entries 1–6). In addition, substituents on the binaphthol moiety are not beneficial for this substrate (entries 5 and 6). The highest selectivity of 51% ee is reached with the *o*-tolyl-substituted ligand **1d**. When the performances of phospholes **3a,b** are compared, the more bulky **3a** gives higher selectivity, which is in contrast with the ligand effects observed in the alkylation of **6**. We speculate that the smaller

**Table 5.** Pd-Catalyzed Allylic Alkylation of **10** with Ligands **1** and **3**<sup>a</sup>

entry	ligand	conv. (%) <sup>b</sup>	ee (%) <sup>c</sup>
1	<b>1a</b> (R = Ph, R' = H)	73	<1
2	<b>1b</b> (R = <i>i</i> -Pr, R' = H)	94	19
3	<b>1c</b> (R = Cy, R' = H)	82	26
4	<b>1d</b> (R = <i>o</i> -Tol, R' = H)	100	44
5	<b>1e</b> (R = Ph, R' = SiMe <sub>3</sub> )	15	50
6	<b>1f</b> (R = <i>i</i> -Pr, R' = Me)	12	38
7	<b>3a</b> (R <sup>1</sup> = Ph, R <sup>2</sup> = H)	6	<1
8	<b>3b</b> (R <sup>1</sup> = H, R <sup>2</sup> = Me)	34	7

<sup>a</sup> Conditions: 0.5 mol % of [Pd<sub>2</sub>(η<sup>3</sup>-C<sub>3</sub>H<sub>5</sub>)<sub>2</sub>Cl<sub>2</sub>], 1.1 mol % of ligand, CH<sub>2</sub>Cl<sub>2</sub>, room temperature, 3 equiv of dimethyl malonate, 3 equiv of BSA, pinch of KOAc. <sup>b</sup> Conversion percentage of acetate after 1 h, determined by GC. <sup>c</sup> Enantiomeric excess, determined by chiral GC (Supelco β-DEX 225).

**Table 6.** Pd-Catalyzed Allylic Alkylation of **12** with Ligands **1** and **3**<sup>a</sup>

entry	ligand	conv. (%) <sup>b</sup>	<b>13/14</b> <sup>c</sup>	ee (%) <sup>d</sup>
1	<b>1a</b> (R = Ph, R' = H)	100	9/91	12
2	<b>1b</b> (R = <i>i</i> -Pr, R' = H)	100	5/95	<5
3	<b>1c</b> (R = Cy, R' = H)	100	5/95	<5
4	<b>1d</b> (R = <i>o</i> -Tol, R' = H)	100	14/86	81
5	<b>1e</b> (R = Ph, R' = SiMe <sub>3</sub> )	100	11/89	<5
6	<b>1f</b> (R = <i>i</i> -Pr, R' = Me)	100	5/95	10
7	<b>3a</b> (R <sup>1</sup> = Ph, R <sup>2</sup> = H)	80	10/90	<5
8	<b>3b</b> (R <sup>1</sup> = H, R <sup>2</sup> = Me)	100	7/93	<5

<sup>a</sup> Conditions: 0.5 mol % of [Pd<sub>2</sub>(η<sup>3</sup>-C<sub>3</sub>H<sub>5</sub>)<sub>2</sub>Cl<sub>2</sub>], 1.1 mol % of ligand, CH<sub>2</sub>Cl<sub>2</sub>, room temperature, 3 equiv of dimethyl malonate, 3 equiv of BSA, pinch of KOAc. <sup>b</sup> Conversion percentage of acetate after 1 h, determined by GC. <sup>c</sup> Branched-to-linear ratio, determined by GC. <sup>d</sup> Enantiomeric excess, determined by chiral HPLC (Chiralcel-OJH).

Me substituents of **8** require a catalyst containing more steric bulk compared to **6** to achieve efficient enantioselection.

Cyclic substrates are usually more difficult to alkylate with high enantioselectivity. The small *syn* substituents, a proton in most cases, poorly interact with the chiral steric environment imposed by the ligand. Indeed, very low enantioselectivities are obtained for most ligands in the allylic alkylation of 3-acetoxycyclohexene (**10**) (Table 5). Only bulky ligands **1d–f** are able to induce significant enantioselection up to 50% ee (entries 4–6).

Monosubstituted linear substrates represent a challenge in allylic alkylations, as both the regio- and enantioselectivity have to be controlled. In contrast to Ir-catalyzed allylic alkylations,<sup>23</sup> Pd-based catalysts give generally low branched to linear ratios (*b/l*).<sup>24</sup> Ligands **1** and **3** provide active catalysts for the allylic alkylation of cinnamyl acetate **12** (Table 6). As expected for Pd-based systems, the branched product **13** is formed in only 5–14% yield and low ee, except for ligand **1d**. A good enantioselectivity of 81% ee at a *b/l* of 14/86 is obtained by using the *o*-tolyl-substituted INDOLPhos ligand **1d** (entry 4). Although the *b/l* is low, the enantioselectivity is among the

highest reported to date and represents a lead for further optimization.<sup>25</sup>

When the efficiency of INDOLPhos(phole) ligands in the asymmetric allylic alkylation is compared to that of other hybrid ligand systems such as phosphite–phosphoramidites, it can be noted that our system is less active.<sup>17b,c</sup> The lower reactivity can be explained in terms of electronic effects. Phosphines are less π-acidic compared to phosphites, which leads to lower reaction rates, as the rate-limiting step is reductive nucleophilic attack.<sup>16</sup> With respect to the enantioselectivity, INDOLPhos-(phole) systems give ee's similar to those for phosphite–phosphoramidite ligands containing a rigid pyranoside sugar backbone.<sup>17b</sup> Phosphite–phosphoramidite ligands containing a more simple amino alcohol backbone, on the other hand, are more selective than our system.<sup>17c</sup> These results indicate that a more flexible backbone is beneficial for the enantioselectivity.

**Mechanism of Enantiodiscrimination.** It is known that, in the case of 1,3-disubstituted substrates, enantiodiscrimination results from preferential attack on one of the enantiotopic termini of the allylpalladium complex.<sup>15b</sup> In the case of ligand **1a**, Pd–allyl complex **4b** is the actual intermediate in the catalytic cycle. As the structure in solution was assigned with NOESY and DFT calculations (Figure 5), and no *syn*–*anti* interconversion was observed, attack on this complex determines which enantiomer is obtained. The other rotational isomer is observed in trace amounts by NMR, and DFT calculations in the gas phase indicate that it would be 0.5 kcal mol<sup>-1</sup> higher in energy. Even though it is present in trace amount, it cannot be excluded that this second rotational isomer plays a role in the reaction, as it is known that species which are present in only very low amount can carry out most of the reaction flux.

The stereochemical pathway of the reaction can be described in terms of the diagram depicted in Scheme 5.<sup>26</sup> Nucleophilic attack can take place on either the major or minor Pd–allyl complex. For the major isomer, rotation accompanied by formation of the η<sup>2</sup>-alkene species favors pathway b toward the *S* enantiomer. The steric bulk of the bisnaphthol hinders the substrate rotation by having unfavorable steric interactions with the newly formed tertiary substituent in the case of path a. If, on the other hand, nucleophilic attack occurs on the minor isomer, no preferred sense of rotation would be expected on steric grounds.

Experimentally, we found that the *S* enantiomer of the alkylation product was formed in excess with all ligands. The selective isomerization and crystal structure of **4a** indicate a labilization of the Pd–C<sub>3</sub> bond (vide supra). These observations support a mechanism following path b: i.e., attack on the C<sub>3</sub> allyl terminus of the major allyl isomer. This mechanism is in agreement with an early as well as a late transition state model. The former is supported by the labilization of the Pd–C<sub>3</sub> bond and the latter by repulsive steric interactions during rotation of the substrate upon nucleophilic attack.<sup>27</sup> If the main reaction flux is carried out by the minor allyl isomer, a much lower enantiomeric excess would be expected, as rotation of the substrate in both cases (paths c and d) is not predominantly hindered by repulsive steric interactions. Therefore, we believe that formation of the alkylation product proceeds by path b.

(25) Pretot, R.; Pfaltz, A. *Angew. Chem., Int. Ed.* **1998**, *37*, 323–325.

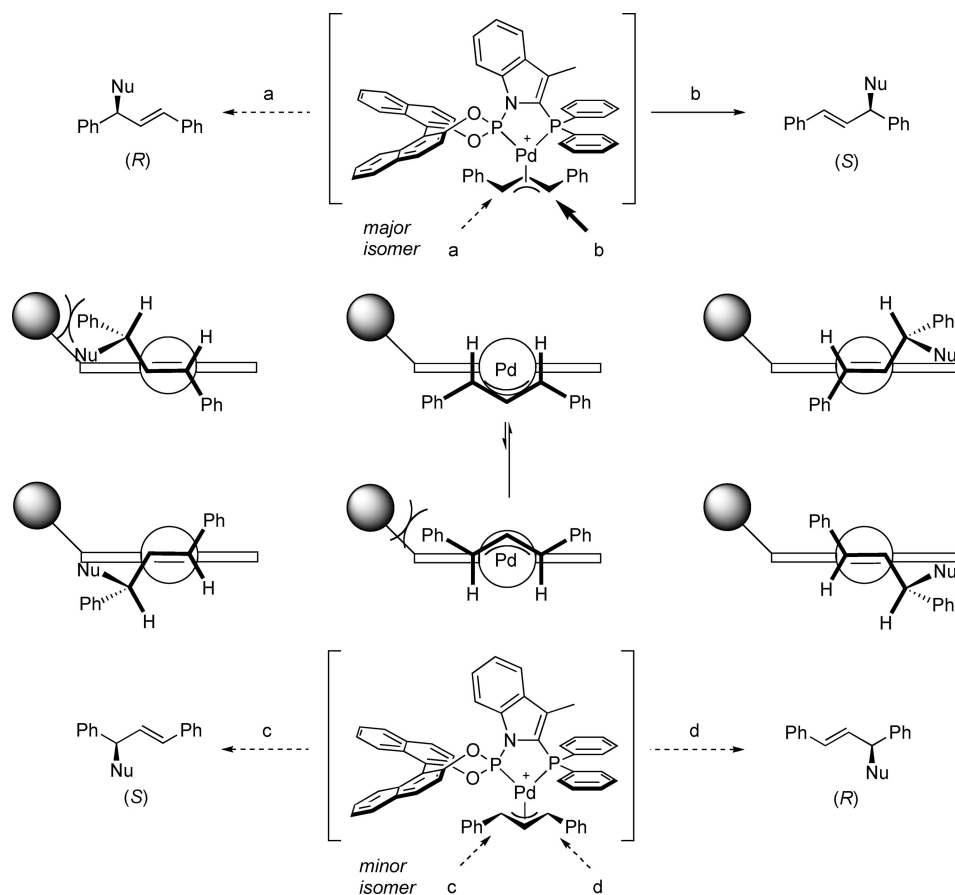
(26) von Matt, P.; Lloyd-Jones, G. C.; Minidis, A. B. E.; Pfaltz, A.; Macko, L.; Neuburger, M.; Zehnder, M.; Rüegger, H.; Pregosin, P. S. *Helv. Chim. Acta* **1995**, *78*, 265–284.

(27) van Leeuwen, P. W. N. M. In *Homogeneous Catalysis, Understanding the Arr*; Kluwer: Dordrecht, The Netherlands, 2004; pp 273–281.

(23) Helmchen, G.; Dahnz, A.; Dubon, P.; Schelwies, M.; Weihofen, R. *Chem. Commun.* **2007**, 675–691.

(24) For a review on Pd-catalyzed asymmetric allylic alkylation of mono-substituted substrates, see: Lu, Z.; Ma, S. M. *Angew. Chem., Int. Ed.* **2008**, *47*, 258–297.

Scheme 5. Enantiocontrol Provided by INDOLPhos(phole) Pd Catalysts



## Conclusions

Phosphole-substituted INDOLPhos derivatives **3a,b** have been successfully synthesized and characterized. For **3b**, the coordination to palladium(II) was investigated in the palladium–allyl complex **5** and compared to the corresponding INDOLPhos palladium species **4a**. In solution these complexes each exist as two isomers in a 1:1 ratio, which interconvert through a  $\eta^3\text{--}\eta^1\text{--}\eta^3$  isomerization. A selective isomerization was found for **4a**, where Pd–C bond opening only occurs trans with regard to the diphenylphosphine donor group, due to steric effects. For complex **5**, no such selectivity has been found, which is explained by the smaller phosphole substituent. As a result, the steric demands of phosphole and phosphoramidite are similar, and Pd–C bond opening occurs at both allyl termini. The rate constant of the isomerization process for **5** is  $k = 3.6\text{ s}^{-1}$ . **4a** does not display dynamic behavior at room temperature, and consequently its rate constant could not be determined.

In the solid state, complexes **4a** and **5** display disorder in the coordinated allyl fragments, confirming the rotational isomerism observed in solution. Interestingly, the phosphole-containing complex **5** forms a tetrameric box structure in the solid state, which is templated by encapsulation of one  $\text{PF}_6$  counteranion. The encapsulation is driven by eight C–H $\cdots$ F interactions between hydrogen atoms located on the phosphole ligand and the  $\text{PF}_6$  anion.

INDOLPhospholes **3a,b** and INDOLPhos ligands **1a–f** were evaluated in the Pd-catalyzed asymmetric allylic alkylation. For 1,3-disubstituted propenyl acetates, high activity was found along with good enantioselectivity up to 90% ee. For cyclic substrate **10**, only moderate ee up to 50% was obtained. The alkylation of cinnamyl acetate was achieved in good enantio-

selectivity, up to 81% ee, but in a low *b/l* of 14/86. The results show that hybrid ligands are able to induce moderate to good enantioselectivities for a range of substrates in the asymmetric allylic alkylation. The introduction of phosphole-containing ligands did not lead to an increase in selectivity, which was anticipated on the basis of the earlier successful application of phospholes in the allylic substitution.

On the basis of the structural data for complexes **4a,b**, the formation of the *S* enantiomer in the case of 1,3-diphenylprop-2-enyl acetate can be rationalized by a selective nucleophilic attack cis to the phosphine in the Pd–allyl intermediate. In contrast to the case for other  $C_1$ -symmetrical ligands possessing two different donor atoms, such as P–N ligands, the ratio of isomeric Pd–allyl intermediates observed in solution is much larger in our case (>50:1 vs 9:1).<sup>28</sup> Analogously, however, the enantioselectivity arises from the regioselective attack on the major isomeric Pd–allyl complex. Our results from X-ray crystallography and 2-D NMR spectrometry indicate that steric rather than electronic effects play the dominant role in this step.

## Experimental Section

**General Considerations.** All reactions were carried out under an atmosphere of argon using standard Schlenk techniques. With the exception of the compounds given below, all reagents were purchased from commercial suppliers and used without further purification. The following compounds were synthesized according to published procedures: phosphorochloridite of (*S*)-(–)-2,2'-

bisnaphthol,<sup>29</sup> 1-cyano-3,4-dimethylphosphole,<sup>30</sup> 1-cyano-2,5-diphenylphosphole,<sup>14b</sup> [Pd<sub>2</sub>(η<sup>3</sup>-1,3-diphenylallyl)<sub>2</sub>Cl<sub>2</sub>],<sup>26</sup> *rac*-1,3-diphenylprop-2-enyl acetate (**6**),<sup>31</sup> *rac*-1,3-dimethylprop-2-enyl acetate (**8**),<sup>32</sup> and *rac*-3-acetoxycyclohexene (**10**).<sup>33</sup> THF, pentane, hexane, and diethyl ether were distilled from sodium benzophenone ketyl; CH<sub>2</sub>Cl<sub>2</sub>, MeCN, EtOAc, *i*-PrOH, and MeOH were distilled from CaH<sub>2</sub>, and toluene was distilled from sodium under nitrogen. Melting points were recorded on a Gallenkamp melting point apparatus and are uncorrected. NMR spectra (<sup>1</sup>H, <sup>31</sup>P, and <sup>13</sup>C) were measured on a Varian INOVA 500 MHz or a Varian MERCURY 300 MHz spectrometer. Optical rotations were determined on a Perkin-Elmer 241 polarimeter. High-resolution mass spectra were recorded on a JEOL JMS SX/SX102A four-sector mass spectrometer; for FAB-MS 3-nitrobenzyl alcohol was used as the matrix. Gas chromatographic analyses were run on a Shimadzu GC-17A apparatus. Chiral GC separations were conducted on an Interscience Focus GC Ultra instrument. Chiral HPLC separations were conducted on a Shimadzu 10A HPLC instrument, equipped with a UV detector.

**Synthesis of Indolylphosphole 2a.** To a solution of 3-methylindole (126 mg, 0.96 mmol) in THF (5 mL) was added dropwise 0.40 mL of *n*-BuLi (2.5 M in hexanes) at -70 °C. The resulting suspension was stirred at -70 °C for 20 min. Carbon dioxide was bubbled through the suspension for 10 min to give a clear pale yellow solution that was warmed to room temperature, after which the solvent was removed in vacuo. The resulting white residue was dissolved in THF (5 mL) to give a clear pale yellow solution, which was cooled to -70 °C. To this solution was added 0.63 mL of *t*-BuLi (1.6 M in pentanes), and the resulting orange solution was stirred at -70 °C for 30 min. To this solution was added a solution of 1-cyano-2,5-diphenylphosphole (250 mg, 0.96 mmol) in THF (2 mL), and the reaction mixture was stirred for 1 h at -70 °C. The resulting yellow solution was warmed to room temperature and stirred for 16 h, after which it was washed with 5 mL of degassed saturated aqueous NH<sub>4</sub>Cl. The organic layer was dried over MgSO<sub>4</sub> and filtered, and the solvent was removed in vacuo to yield the product as a bright yellow solid. Yield: 293 mg (84%). Mp: 144 °C. <sup>1</sup>H NMR (CDCl<sub>3</sub>, 499.8 MHz, 298 K): δ (ppm) 7.57 (m, 5H), 7.51 (br s, 1H), 7.42 (d, *J*<sub>P,H</sub> = 11.0 Hz, 2H), 7.29 (t, *J*<sub>H,H</sub> = 7.5 Hz, 4H), 7.20 (t, *J*<sub>H,H</sub> = 7.5 Hz, 2H), 7.13 (m, 2H), 7.07 (m, 1H), 2.76 (s, 3H). <sup>13</sup>C NMR (CDCl<sub>3</sub>, 125.7 MHz, 298 K): δ (ppm) 150.29 (C<sub>q</sub>), 138.46 (C<sub>q</sub>), 136.20 (C<sub>q</sub>, *J*<sub>P,C</sub> = 16.5 Hz), 132.76 (CH, *J*<sub>P,C</sub> = 10.2 Hz), 129.04 (CH), 127.79 (CH), 126.36 (CH, *J*<sub>P,C</sub> = 9.2 Hz), 124.25 (C<sub>q</sub>), 124.01 (C<sub>q</sub>), 123.72 (CH), 121.56 (C<sub>q</sub>, *J*<sub>P,C</sub> = 16.5 Hz), 119.52 (CH), 119.28 (CH), 111.05 (CH), 10.47 (CH<sub>3</sub>, *J*<sub>P,C</sub> = 10.6 Hz). <sup>31</sup>P{<sup>1</sup>H} NMR (CDCl<sub>3</sub>, 202.3 MHz, 298 K): δ (ppm) -32.25 (s). HRMS (FAB): *m/z* calcd for [M + H]<sup>+</sup> C<sub>25</sub>H<sub>21</sub>NP 366.1412, found 366.1414.

**Synthesis of Indolylphosphole 2b.** The same procedure was followed as for **2a**, except for using 1-cyano-3,4-dimethylphosphole (208 mg, 1.52 mmol) instead of 1-cyano-2,5-diphenylphosphole and 200 mg of 3-methylindole (1.52 mmol) to give the product as an off-white solid. Yield: 262 mg (71%). Mp: 117 °C. <sup>1</sup>H NMR (CDCl<sub>3</sub>, 499.8 MHz, 298 K): δ (ppm) 7.58 (d, *J*<sub>H,H</sub> = 8.0 Hz, 1H), 7.41 (br s, 1H), 7.21 (m, 2H), 7.11 (t, *J*<sub>H,H</sub> = 7.0 Hz, 1H), 6.47 (d, *J*<sub>P,H</sub> = 38.5 Hz, 2H), 2.58 (s, 3H), 2.21 (d, *J*<sub>P,H</sub> = 3.5 Hz, 6H). <sup>13</sup>C NMR (CDCl<sub>3</sub>, 125.7 MHz, 298 K): δ (ppm) 150.45 (C<sub>q</sub>), 150.38 (C<sub>q</sub>), 137.93 (C<sub>q</sub>), 129.11 (CH), 123.47 (CH), 122.90 (C<sub>q</sub>, *J*<sub>P,C</sub> =

29.0 Hz), 122.03 (C<sub>q</sub>, *J*<sub>P,C</sub> = 21.1 Hz), 121.95 (CH, *J*<sub>P,C</sub> = 33.3 Hz), 119.29 (CH), 110.77 (CH), 18.07 (CH<sub>3</sub>, *J*<sub>P,C</sub> = 3.8 Hz), 10.16 (CH<sub>3</sub>, *J*<sub>P,C</sub> = 10.6 Hz). <sup>31</sup>P{<sup>1</sup>H} NMR (CDCl<sub>3</sub>, 202.3 MHz, 298 K): δ (ppm) -37.70 (s). HRMS (FAB): *m/z* calcd for [M + H]<sup>+</sup> C<sub>15</sub>H<sub>17</sub>NP 242.1099, found 242.1093.

**Synthesis of INDOLPhosphole 3a.** To a solution of indolylphosphole **2a** (70 mg, 0.19 mmol) in THF (3 mL) was added dropwise 0.76 mL of *n*-BuLi (0.25 M in hexanes) at -70 °C. The resulting orange solution was stirred for 10 min at -70 °C. To this solution was added a solution of (*S*)-(-)-2,2'-bisanaphthol phosphorochloridite (67 mg, 0.19 mmol) in THF (1 mL) at -70 °C. The reaction mixture was stirred for 1 h at -70 °C and then warmed to room temperature. The resulting yellow solution was filtered through a plug of SiO<sub>2</sub> and concentrated in vacuo. The crude product was further purified by SiO<sub>2</sub> chromatography (5% EtOAc/hexane) to give a bright yellow solid. Yield: 81 mg (63%). Mp: 147 °C. [α]<sub>D</sub><sup>20</sup> = +36.0° (*c* = 0.5, CHCl<sub>3</sub>). <sup>1</sup>H NMR (CDCl<sub>3</sub>, 499.8 MHz, 298 K): δ (ppm) 8.01–7.92 (m, 3H), 7.71 (d, *J*<sub>H,H</sub> = 7.0 Hz, 1H), 7.60 (d, *J*<sub>H,H</sub> = 7.5 Hz, 4H), 7.53 (d, *J*<sub>H,H</sub> = 8.0 Hz, 1H), 7.50–7.22 (m, 15H), 6.81 (t, *J*<sub>H,H</sub> = 7.5 Hz, 1H), 6.21 (br s, 1H), 6.11 (t, *J*<sub>H,H</sub> = 8.0 Hz, 1H), 5.55 (br s, 1H), 2.92 (br s, 3H). <sup>13</sup>C NMR (CDCl<sub>3</sub>, 125.7 MHz, 298 K): δ (ppm) 150.09 (C<sub>q</sub>, *J*<sub>P,C</sub> = 4.7 Hz), 148.73 (C<sub>q</sub>), 136.87 (C<sub>q</sub>, *J*<sub>P,C</sub> = 16.0 Hz), 133.13 (C<sub>q</sub>), 132.80 (C<sub>q</sub>), 131.95 (C<sub>q</sub>), 131.43 (C<sub>q</sub>), 130.81 (CH), 130.48 (CH), 129.07 (CH), 129.01 (CH), 128.56 (CH, *J*<sub>P,C</sub> = 22.4 Hz), 127.48 (CH), 127.35 (CH), 126.88 (CH, *J*<sub>P,C</sub> = 9.7 Hz), 126.75 (CH), 126.62 (CH), 126.37 (CH), 125.49 (CH), 125.01 (CH), 122.94 (C<sub>q</sub>), 121.91 (CH), 121.15 (CH), 121.01 (CH), 119.20 (CH), 116.16 (CH), 111.03 (CH), 11.40 (CH<sub>3</sub>). <sup>31</sup>P{<sup>1</sup>H} NMR (CDCl<sub>3</sub>, 202.3 MHz, 298 K): δ (ppm) 148.57 (s), -32.66 (s). HRMS (FAB): *m/z* calcd for [M + H]<sup>+</sup> C<sub>45</sub>H<sub>32</sub>N<sub>2</sub>O<sub>2</sub>P<sub>2</sub> 680.1908, found 680.1906.

**Synthesis of INDOLPhosphole 3b.** The same procedure was followed as for **3a**, except for using indolylphosphine **2b** (70 mg, 0.29 mmol) instead of **2a**, 1.16 mL of *n*-BuLi (0.25 M in hexanes), and 102 mg of (*S*)-(-)-2,2'-bisanaphthol phosphorochloridite (0.29 mmol) to give the product as a white solid. Yield: 77 mg (48%). Mp: 167 °C. [α]<sub>D</sub><sup>20</sup> = +188.0° (*c* = 0.5, CHCl<sub>3</sub>). <sup>1</sup>H NMR (CDCl<sub>3</sub>, 499.8 MHz, 298 K): δ (ppm) 8.02 (d, *J*<sub>H,H</sub> = 8.5 Hz, 1H), 7.97 (d, *J*<sub>H,H</sub> = 8.0 Hz, 1H), 7.81 (d, *J*<sub>H,H</sub> = 8.0 Hz, 1H), 7.52 (dd, *J*<sub>H,H</sub> = 9.0 Hz, *J*<sub>H,H</sub> = 4.0 Hz, 2H), 7.50–7.43 (m, 4H), 7.37 (d, *J*<sub>H,H</sub> = 8.0 Hz, 1H), 7.34–7.30 (m, 2H), 6.82 (m, 2H), 6.76–6.68 (m, 2H), 6.39 (d, *J*<sub>H,H</sub> = 8.5 Hz, 1H), 6.15 (t, *J*<sub>H,H</sub> = 8.0 Hz, 1H), 2.49 (s, 3H), 2.12 (br s, 6H). <sup>13</sup>C NMR (CDCl<sub>3</sub>, 125.7 MHz, 298 K): δ (ppm) 150.64 (C<sub>q</sub>, *J*<sub>P,C</sub> = 5.5 Hz), 148.98 (C<sub>q</sub>), 141.09 (C<sub>q</sub>, *J*<sub>P,C</sub> = 7.5 Hz), 133.22 (C<sub>q</sub>), 132.94 (C<sub>q</sub>), 131.91 (C<sub>q</sub>), 131.52 (C<sub>q</sub>), 130.84 (CH), 130.55 (CH), 129.92 (C<sub>q</sub>, *J*<sub>P,C</sub> = 27.0 Hz, *J*<sub>P,C</sub> = 5.0 Hz), 129.18 (CH), 128.58 (CH, *J*<sub>P,C</sub> = 10.9 Hz), 127.40 (CH), 126.89 (CH), 126.63 (CH), 126.48 (CH), 125.47 (CH), 125.06 (CH), 124.82 (C<sub>q</sub>, *J*<sub>P,C</sub> = 5.9 Hz), 123.81 (CH), 122.92 (C<sub>q</sub>), 121.95 (CH), 121.76 (CH), 121.01 (CH), 118.74 (CH), 116.17 (CH), 18.14 (CH<sub>3</sub>), 10.80 (CH<sub>3</sub>, *J*<sub>P,C</sub> = 14.3 Hz). <sup>31</sup>P{<sup>1</sup>H} NMR (CDCl<sub>3</sub>, 202.3 MHz, 298 K): δ (ppm) 148.33 (d, *J*<sub>P,P</sub> = 43.1 Hz), -37.03 (d, *J*<sub>P,P</sub> = 43.1 Hz). HRMS (FAB): *m/z* calcd for [M + H]<sup>+</sup> C<sub>35</sub>H<sub>28</sub>O<sub>2</sub>N<sub>2</sub>P<sub>2</sub> 556.1595, found 556.1594.

**Synthesis of Complex 4a, [Pd(1a)(C<sub>3</sub>H<sub>5</sub>)<sub>2</sub>]PF<sub>6</sub>.** To a solution of INDOLPhos (**1a**; 100 mg, 0.16 mmol) in CH<sub>2</sub>Cl<sub>2</sub> (4 mL) was added [Pd<sub>2</sub>(η<sup>3</sup>-C<sub>3</sub>H<sub>5</sub>)<sub>2</sub>Cl<sub>2</sub>] (29 mg, 0.08 mmol) at room temperature. The solution was stirred for 5 min. Silver hexafluorophosphate salt (41 mg, 0.16 mmol) was then added, and the resulting suspension was stirred for 30 min. Filtration over Celite and evaporation of the solvent afforded the product as a white solid. Colorless needles suitable for X-ray crystallographic analysis were obtained by slow diffusion of hexanes into a saturated dichloromethane solution. Yield: 117 mg (79%). Mp: 174 °C dec. [α]<sub>D</sub><sup>20</sup> = +263.0° (*c* = 1.0, CHCl<sub>3</sub>). <sup>1</sup>H NMR (CD<sub>2</sub>Cl<sub>2</sub>, 499.8 MHz, 298 K): δ (ppm) 8.34 (d, *J*<sub>H,H</sub> = 9.0 Hz, 0.5H), 8.32 (d, *J*<sub>H,H</sub> = 9.0 Hz, 0.5H), 8.16 (t, *J*<sub>H,H</sub> = 7.5 Hz, 1H), 7.98 (t, *J*<sub>H,H</sub> = 8.5 Hz, 1H), 7.81–7.54 (m,

(29) Buisman, G. J. H.; van der Veen, L. A.; Klootwijk, A.; de Lange, W. G. J.; Kamer, P. C. J.; van Leeuwen, P. W. N. M.; Vogt, D. *Organometallics* **1997**, *16*, 2929–2939.

(30) Holand, S.; Mathy, F. *Organometallics* **1988**, *7*, 1796–1801.

(31) Auburn, P. R.; Mackenzie, P. B.; Bosnich, B. *J. Am. Chem. Soc.* **1985**, *107*, 2033–2046.

(32) Moreno-Mañas, M.; Ribas, J.; Virgili, A. *J. Org. Chem.* **1988**, *53*, 5328–5335.

(33) Jia, C. G.; Muller, P.; Mimoun, H. *J. Mol. Catal. A: Chem.* **1995**, *101*, 127–136.

15H), 7.51–7.43 (m, 4H), 7.12 (t,  $J_{\text{H,H}} = 7.5$  Hz, 1H), 6.86 (d,  $J_{\text{H,H}} = 9.0$  Hz, 0.5H), 6.75 (d,  $J_{\text{H,H}} = 9.0$  Hz, 0.5H), 6.48 (m, 1H), 6.40 (d,  $J_{\text{H,H}} = 8.5$  Hz, 0.5H), 6.37 (d,  $J_{\text{H,H}} = 8.5$  Hz, 0.5H), 5.75 (tt,  $J_{\text{H,H}} = 14.0$  Hz,  $J_{\text{H,H}} = 7.5$  Hz, 0.5H), 5.47 (tt,  $J_{\text{H,H}} = 14.0$  Hz,  $J_{\text{H,H}} = 7.0$  Hz, 0.5H), 4.82 (t,  $J_{\text{H,H}} = 7.5$  Hz, 0.5H), 4.68 (t,  $J_{\text{H,H}} = 8.5$  Hz, 0.5H), 4.58 (m, 0.5H), 4.36 (m, 0.5H), 3.47 (m, 0.5H), 3.33 (t,  $J_{\text{H,H}} = 15.0$  Hz, 0.5H), 3.22 (t,  $J_{\text{H,H}} = 15.0$  Hz, 0.5H), 2.96 (m, 0.5H), 2.09 (s, 3H).  $^{13}\text{C}$  NMR ( $\text{CD}_2\text{Cl}_2$ , 125.7 MHz, 298 K):  $\delta$  (ppm) 149.50 ( $\text{C}_q$ ,  $J_{\text{P,C}} = 6.4$  Hz), 149.39 ( $\text{C}_q$ ,  $J_{\text{P,C}} = 5.9$  Hz), 147.11 ( $\text{C}_q$ ,  $J_{\text{P,C}} = 5.2$  Hz), 146.96 ( $\text{C}_q$ ,  $J_{\text{P,C}} = 5.5$  Hz), 139.18 ( $\text{C}_q$ ), 136.73 ( $\text{C}_q$ ), 133.58 (CH), 133.46 (CH), 133.31 (CH), 133.21 (CH), 133.10 (CH), 133.01 ( $\text{C}_q$ ), 132.96 (CH), 132.91 ( $\text{C}_q$ ), 132.86 (CH), 132.77 (CH), 132.73 ( $\text{C}_q$ ), 132.68 (CH), 132.51 (CH), 132.42 (CH), 130.69 (CH,  $J_{\text{P,C}} = 12.2$  Hz), 130.58 (CH,  $J_{\text{P,C}} = 12.3$  Hz), 130.39 (CH,  $J_{\text{P,C}} = 8.4$  Hz), 130.30 (CH,  $J_{\text{P,C}} = 8.4$  Hz), 129.52 (CH,  $J_{\text{P,C}} = 5.0$  Hz), 129.21 (CH,  $J_{\text{P,C}} = 2.1$  Hz), 128.09 (CH), 128.05 (CH), 127.64 (CH,  $J_{\text{P,C}} = 11.8$  Hz), 127.38 (CH,  $J_{\text{P,C}} = 4.1$  Hz), 127.24 (CH,  $J_{\text{P,C}} = 4.3$  Hz), 127.04 (CH,  $J_{\text{P,C}} = 3.0$  Hz), 126.78 (CH), 125.31 (CH,  $J_{\text{P,C}} = 6.3$  Hz), 125.23 (CH,  $J_{\text{P,C}} = 6.4$  Hz), 124.31 (CH), 124.24 ( $\text{C}_q$ ), 122.46 ( $\text{C}_q$ ), 121.15 (CH), 121.03 (CH), 120.18 (CH,  $J_{\text{P,C}} = 8.0$  Hz), 115.65 (CH), 73.94 ( $\text{CH}_2$ ,  $J_{\text{P,C}} = 44.1$  Hz), 73.89 ( $\text{CH}_2$ ,  $J_{\text{P,C}} = 45.1$  Hz), 73.01 ( $\text{CH}_2$ ,  $J_{\text{P,C}} = 8.2$  Hz), 72.80 ( $\text{CH}_2$ ,  $J_{\text{P,C}} = 8.0$  Hz), 10.93 ( $\text{CH}_3$ ).  $^{31}\text{P}\{^1\text{H}\}$  NMR ( $\text{CD}_2\text{Cl}_2$ , 202.3 MHz, 298 K):  $\delta$  (ppm) 293.13 (septuplet,  $J_{\text{P,F}} = 710.1$  Hz,  $\text{PF}_6$ ), 151.45 (d,  $J_{\text{P,P}} = 83.5$  Hz, 0.5P), 151.42 (d,  $J_{\text{P,P}} = 83.5$  Hz, 0.5P), 16.99 (d,  $J_{\text{P,P}} = 83.5$  Hz, 0.5P), 16.86 (d,  $J_{\text{P,P}} = 82.3$  Hz, 0.5P). HRMS (FAB):  $m/z$  calcd for  $[\text{M} - \text{PF}_6]^+ \text{C}_{44}\text{H}_{34}\text{O}_2\text{NP}_2\text{Pd}$  776.1116, found 776.1119.

**Synthesis of Complex 4b, [Pd(1a)(1,3-diphenylallyl)]PF<sub>6</sub>.** To a solution of INDOLPhos (**1a**; 100 mg, 0.16 mmol) in  $\text{CH}_2\text{Cl}_2$  (5 mL) was added  $[\text{Pd}_2(\eta^3\text{-}1,3\text{-diphenylallyl})_2\text{Cl}_2]$  (53 mg, 0.08 mmol) at room temperature. The solution was stirred for 15 min. Silver hexafluorophosphate salt (41 mg, 0.16 mmol) was then added, and the resulting suspension was stirred for 30 min. Filtration over Celite gave a bright yellow solution. Hexanes (10 mL) was added to precipitate a bright yellow solid. The solvent was removed by syringe, and the product was dried in vacuo. Yield: 103 mg (60%). Mp: 221 °C dec.  $[\alpha]_{\text{D}}^{20} = +420.0^\circ$  ( $c = 1.0$ ,  $\text{CHCl}_3$ ).  $^1\text{H}$  NMR ( $\text{CDCl}_3$ , 499.8 MHz, 298 K):  $\delta$  (ppm) 8.19 (d,  $J_{\text{H,H}} = 9.0$  Hz, 1H), 8.13 (d,  $J_{\text{H,H}} = 9.0$  Hz, 1H), 8.01 (d,  $J_{\text{H,H}} = 8.5$  Hz, 1H), 7.85 (d,  $J_{\text{H,H}} = 8.0$  Hz, 1H), 7.68–7.54 (m, 6H), 7.50 (t,  $J_{\text{H,H}} = 7.5$  Hz, 2H), 7.37–7.22 (m, 8H), 7.05 (d,  $J_{\text{H,H}} = 8.5$  Hz, 1H), 7.02 (t,  $J_{\text{H,H}} = 7.5$  Hz, 2H), 6.94 (t,  $J_{\text{H,H}} = 7.5$  Hz, 1H), 6.90 (d,  $J_{\text{H,H}} = 7.5$  Hz, 2H), 6.81 (m, 3H), 6.65 (d,  $J_{\text{H,H}} = 7.5$  Hz, 1H), 6.63 (d, 7.5 Hz, 1H), 6.26 (m, 3H), 6.19 (d,  $J_{\text{H,H}} = 6.5$  Hz, 1H), 6.17 (m, 1H), 5.93 (d,  $J_{\text{H,H}} = 8.5$  Hz, 1H), 5.77 (vt,  $J = 10.0$  Hz, 1H), 5.60 (vt,  $J = 15.0$  Hz, 1H), 1.84 (s, 3H).  $^{13}\text{C}$  NMR ( $\text{CDCl}_3$ , 125.7 MHz, 298 K):  $\delta$  (ppm) 149.28 ( $\text{C}_q$ ,  $J_{\text{P,C}} = 14.8$  Hz), 147.14 ( $\text{C}_q$ ,  $J_{\text{P,C}} = 5.4$  Hz), 138.62 ( $\text{C}_q$ ,  $J_{\text{P,C}} = 6.7$  Hz), 137.34 ( $\text{C}_q$ ,  $J_{\text{P,C}} = 5.0$  Hz), 136.06 ( $\text{C}_q$ ,  $J_{\text{P,C}} = 4.7$  Hz), 135.48 ( $\text{C}_q$ ,  $J_{\text{P,C}} = 12.7$  Hz), 134.45 (CH), 134.34 (CH), 133.06 (CH), 132.82 ( $\text{C}_q$ ), 132.60 ( $\text{C}_q$ ), 132.54 (CH), 132.05 ( $\text{C}_q$ ), 131.65 (CH,  $J_{\text{P,C}} = 2.5$  Hz), 131.58 (CH), 131.34 (CH,  $J_{\text{P,C}} = 11.8$  Hz), 129.89 (CH,  $J_{\text{P,C}} = 12.2$  Hz), 129.75 ( $\text{C}_q$ ,  $J_{\text{P,C}} = 10.9$  Hz), 129.19 (CH), 129.12 (CH), 128.72 (CH), 128.53 (CH), 128.30 (CH,  $J_{\text{P,C}} = 10.2$  Hz), 127.63 (CH), 127.46 (CH), 127.34 (CH), 126.96 (CH), 126.37 (CH,  $J_{\text{P,C}} = 9.2$  Hz), 126.08 (CH), 125.71 ( $\text{C}_q$ ,  $J_{\text{P,C}} = 20.6$  Hz), 125.70 (CH), 125.31 ( $\text{C}_q$ ,  $J_{\text{P,C}} = 19.4$  Hz), 123.39 (CH), 122.27 ( $\text{C}_q$ ,  $J_{\text{P,C}} = 2.9$  Hz), 121.84 (CH), 121.70 ( $\text{C}_q$ ,  $J_{\text{P,C}} = 2.9$  Hz), 120.37 (CH), 120.11 (CH), 115.65 (CH), 115.52 (CH), 94.21 (CH,  $J_{\text{P,C}} = 36.0$ , 5.9 Hz), 92.06 (CH,  $J_{\text{P,C}} = 24.9$ , 10.1 Hz), 10.45 ( $\text{CH}_3$ ).  $^{31}\text{P}\{^1\text{H}\}$  NMR ( $\text{CDCl}_3$ , 202.3 MHz, 298 K):  $\delta$  (ppm) 293.76 (septuplet,  $J_{\text{P,F}} = 714.1$  Hz,  $\text{PF}_6$ ), 146.02 (d,  $J_{\text{P,P}} = 103.8$  Hz), 12.83 (d,  $J_{\text{P,P}} = 103.8$  Hz); a second set of signals was observed in trace amounts (<2%) at  $\delta$  (ppm) 145.42 (d,  $J_{\text{P,P}} = 108.6$  Hz), 12.42 (d,  $J_{\text{P,P}} = 108.1$  Hz). HRMS (FAB):  $m/z$  calcd for  $[\text{M} - \text{PF}_6]^+ \text{C}_{56}\text{H}_{42}\text{O}_2\text{NP}_2\text{Pd}$  928.1745, found 928.1738.

**Synthesis of Complex 5, [Pd(3b)(C<sub>3</sub>H<sub>5</sub>)<sub>2</sub>]PF<sub>6</sub>.** To a solution of INDOLPhosphole (**3b**; 28.0 mg, 0.050 mmol) in  $\text{CH}_2\text{Cl}_2$  (2 mL) was added  $[\text{Pd}_2(\eta^3\text{-C}_3\text{H}_5)_2\text{Cl}_2]$  (9.2 mg, 0.025 mmol) at room temperature. The solution was stirred for 15 min. Silver hexafluorophosphate salt (12.7 mg, 0.050 mmol) was then added, and the resulting suspension was stirred for 30 min. Filtration over Celite and evaporation of the solvent afforded the product as a white solid. Needles suitable for X-ray crystallographic analysis were obtained by slow diffusion of hexanes into a saturated dichloromethane solution. Yield: 42 mg (99%). Mp: 166 °C dec.  $[\alpha]_{\text{D}}^{20} = +354.0^\circ$  ( $c = 0.5$ ,  $\text{CHCl}_3$ ).  $^1\text{H}$  NMR ( $\text{CD}_2\text{Cl}_2$ , 499.8 MHz, 263 K):  $\delta$  (ppm) 8.29 (d,  $J_{\text{H,H}} = 9.0$  Hz, 0.5H), 8.26,  $J_{\text{H,H}} = 9.0$  Hz, 0.5H), 8.13 (t,  $J_{\text{H,H}} = 8.5$  Hz, 1H), 7.99 (t,  $J_{\text{H,H}} = 7.5$  Hz, 1H), 7.80 (d,  $J_{\text{H,H}} = 9.0$  Hz, 0.5H), 7.76 (d,  $J_{\text{H,H}} = 9.0$  Hz, 0.5H), 7.72 (d,  $J_{\text{H,H}} = 9.0$  Hz, 0.5H), 7.65–7.58 (m, 2H), 7.52–7.42 (m, 5H), 7.06 (t,  $J_{\text{H,H}} = 8.5$  Hz, 2H), 6.67–6.44 (m, 2H), 6.42 (t,  $J_{\text{H,H}} = 7.5$  Hz, 1H), 6.18 (d,  $J_{\text{H,H}} = 8.5$  Hz, 0.5H), 6.14 (d,  $J_{\text{H,H}} = 8.5$  Hz, 0.5H), 5.62 (tt,  $J_{\text{H,H}} = 13.5$  Hz,  $J_{\text{H,H}} = 7.0$  Hz, 0.5H), 4.34 (m, 1H), 4.26 (t,  $J_{\text{H,H}} = 9.0$  Hz, 0.5H), 4.16 (m, 0.5H), 3.28 (m, 1H), 3.12 (t,  $J_{\text{H,H}} = 15.0$  Hz, 0.5H), 2.89 (m, 0.5H), 2.35 (s, 1.5H), 2.34 (s, 1.5H), 2.32 (s, 3H), 2.04 (s, 3H).  $^{13}\text{C}$  NMR ( $\text{CD}_2\text{Cl}_2$ , 125.7 MHz, 298 K):  $\delta$  (ppm) 156.24 ( $\text{C}_q$ ), 150.01 ( $\text{C}_q$ ), 147.63 ( $\text{C}_q$ ), 139.09 ( $\text{C}_q$ ), 136.64 ( $\text{C}_q$ ), 133.30 ( $\text{C}_q$ ), 132.95 ( $\text{C}_q$ ), 132.87 ( $\text{C}_q$ ), 132.68 ( $\text{C}_q$ ), 132.59 (CH), 129.51 (CH), 129.21 (CH), 128.04 (CH), 127.65 (CH), 127.45 (CH), 127.22 (CH), 127.00 (CH), 126.15 (CH), 124.84 (CH), 124.41 ( $\text{C}_q$ ), 124.09 (CH), 122.44 ( $\text{C}_q$ ), 121.03 (CH), 120.82 (CH), 120.46 (CH), 120.14 (CH), 119.32 (CH), 115.63 (CH), 73.89 ( $\text{CH}_2$ ), 73.15 ( $\text{CH}_2$ ), 18.22 ( $\text{CH}_3$ ), 8.92 ( $\text{CH}_3$ ).  $^{31}\text{P}\{^1\text{H}\}$  NMR ( $\text{CD}_2\text{Cl}_2$ , 202.3 MHz, 263 K):  $\delta$  (ppm) 292.94 (septuplet,  $J_{\text{P,F}} = 711.5$  Hz,  $\text{PF}_6$ ), 151.28 (d,  $J_{\text{P,P}} = 74.5$  Hz, 0.5P), 151.17 (d,  $J_{\text{P,P}} = 75.1$  Hz, 0.5P), 3.59 (d,  $J_{\text{P,P}} = 75.1$  Hz, 0.5P), 3.47 (d,  $J_{\text{P,P}} = 74.4$  Hz, 0.5P). HRMS (FAB):  $m/z$  calcd for  $[\text{M} - \text{PF}_6]^+ \text{C}_{38}\text{H}_{32}\text{O}_2\text{NP}_2\text{Pd}$  702.0958, found 702.0950.

**Allylic Alkylation of *rac*-1,3-Diphenylprop-3-enyl Acetate (6).** A solution of  $[\text{Pd}_2(\eta^3\text{-C}_3\text{H}_5)_2\text{Cl}_2]$  (0.46 mg, 1.25  $\mu\text{mol}$ ) and INDOLPhos(phole) ligand (2.75  $\mu\text{mol}$ ) in  $\text{CH}_2\text{Cl}_2$  (1 mL) was stirred for 30 min. Subsequently, a solution of *rac*-**6** (63 mg, 0.25 mmol) in  $\text{CH}_2\text{Cl}_2$  (1 mL), dimethyl malonate (86  $\mu\text{L}$ , 0.75 mmol), *N,O*-bis(trimethylsilyl)acetamide (185  $\mu\text{L}$ , 0.75 mmol), and a pinch of KOAc were added. The reaction mixture was stirred at room temperature. After 1 h the reaction mixture was diluted with  $\text{Et}_2\text{O}$  (3 mL) and saturated aqueous  $\text{NH}_4\text{Cl}$  (10 mL). The aqueous phase was removed. To determine the conversion, a sample for GC analysis was taken from the organic phase. The solvent was removed in vacuo. To determine the ee by HPLC (Chiralcel-ODH, 0.5% 2-propanol/hexane, flow 0.5 mL/min), a sample was filtered over  $\text{SiO}_2$ , using hexanes as eluent.

**Allylic Alkylation of *rac*-1,3-Dimethylprop-3-enyl Acetate (8).** A solution of  $[\text{Pd}_2(\eta^3\text{-C}_3\text{H}_5)_2\text{Cl}_2]$  (0.46 mg, 1.25  $\mu\text{mol}$ ) and INDOLPhos(phole) ligand (2.75  $\mu\text{mol}$ ) in  $\text{CH}_2\text{Cl}_2$  (1 mL) was stirred for 30 min. Subsequently, a solution of *rac*-**8** (32 mg, 0.25 mmol) in  $\text{CH}_2\text{Cl}_2$  (1 mL), dimethyl malonate (86  $\mu\text{L}$ , 0.75 mmol), *N,O*-bis(trimethylsilyl)acetamide (185  $\mu\text{L}$ , 0.75 mmol), and a pinch of KOAc were added. The reaction mixture was stirred at room temperature. After 1 h the reaction mixture was diluted with  $\text{Et}_2\text{O}$  (3 mL) and saturated aqueous  $\text{NH}_4\text{Cl}$  (10 mL). The aqueous phase was removed. Conversion and ee were determined by chiral GC (Chiralcel DEX CB, isothermal at 65 °C).

**Allylic Alkylation of *rac*-3-Acetoxy-cyclohexene (10).** A solution of  $[\text{Pd}_2(\eta^3\text{-C}_3\text{H}_5)_2\text{Cl}_2]$  (0.46 mg, 1.25  $\mu\text{mol}$ ) and INDOLPhos(phole) ligand (2.75  $\mu\text{mol}$ ) in  $\text{CH}_2\text{Cl}_2$  (1 mL) was stirred for 30 min. Subsequently, a solution of *rac*-**10** (35 mg, 0.25 mmol) in  $\text{CH}_2\text{Cl}_2$  (1 mL), dimethyl malonate (86  $\mu\text{L}$ , 0.75 mmol), *N,O*-bis(trimethylsilyl)acetamide (185  $\mu\text{L}$ , 0.75 mmol), and a pinch of KOAc were added. The reaction mixture was stirred at room temperature. After 1 h the reaction mixture was diluted with  $\text{Et}_2\text{O}$  (3 mL) and saturated aqueous  $\text{NH}_4\text{Cl}$  (10 mL). The aqueous phase was removed.

Conversion and ee were determined by chiral GC (Supelco  $\beta$ -DEX 225, isothermal at 50 °C for 2 min, 3 °C/min to 190 °C).

**Allylic Alkylation of Cinnamyl Acetate (12).** A solution of  $[\text{Pd}_2(\eta^3\text{-C}_3\text{H}_5)_2\text{Cl}_2]$  (0.46 mg, 1.25  $\mu\text{mol}$ ) and INDOLPhos(phole) ligand (2.75  $\mu\text{mol}$ ) in  $\text{CH}_2\text{Cl}_2$  (1 mL) was stirred for 30 min. Subsequently, a solution of **12** (42  $\mu\text{L}$ , 0.25 mmol) in  $\text{CH}_2\text{Cl}_2$  (1 mL), dimethyl malonate (86  $\mu\text{L}$ , 0.75 mmol), *N,O*-bis(trimethylsilyl)acetamide (185  $\mu\text{L}$ , 0.75 mmol), and a pinch of KOAc were added. The reaction mixture was stirred at room temperature. After 1 h the reaction mixture was diluted with  $\text{Et}_2\text{O}$  (3 mL) and saturated aqueous  $\text{NH}_4\text{Cl}$  (10 mL). The aqueous phase was removed. To determine the conversion, a sample for GC analysis was taken from the organic phase. The solvent was removed in vacuo. To determine the ee by HPLC (Chiralcel-OJH, 3.0% 2-propanol/hexane, flow 0.7 mL/min) a sample was filtered over  $\text{SiO}_2$ , using hexanes as eluent.

**X-ray Crystallography of 4a and 5.** All reflection intensities were measured at 110(2) K using a Nonius KappaCCD diffractometer (rotating anode) with graphite-monochromated Mo K $\alpha$  radiation ( $\lambda = 0.71073$  Å) under the program COLLECT.<sup>34</sup> The program PEAKREF<sup>35</sup> was used to refine the cell dimensions. Data reduction was done using the program EVALCCD.<sup>36</sup> The structure of **4a** was solved with the program DIRDIF08<sup>37</sup> and that of **5** with the program SHELXS-97.<sup>38</sup> The two structures were refined on  $F^2$  with SHELXL-97.<sup>38</sup> Analytical absorption corrections based on crystal face indexing were applied to the data using SADABS<sup>39</sup> (transmission ranges: for **4a**, 0.80–0.92; for **5**, 0.87–1.00). The temperature of the data collection was controlled using the Oxford Cryostream 600 system (manufactured by Oxford Cryosystems). The H atoms were placed at calculated positions (AFIX 23 or AFIX 43 or AFIX 93 or AFIX 137) with isotropic displacement parameters having values 1.2 or 1.5 times the  $U_{\text{eq}}$  value of the attached C atom and were refined with a riding model. In the crystal structure of **4a**, the asymmetric unit contains two crystallographically independent Pd complexes, two hexafluorophosphate counteranions, and two dichloromethane solvent molecules. The allyl ligands are disordered, and their major components were refined to 0.703(8) and 0.623(9). In the crystal structure of **5**, the asymmetric unit was modeled with four Pd complexes, four hexafluorophosphate counteranions, and two dichloromethane solvent molecules. One allyl ligand and one  $\text{PF}_6^-$  counteranion were found to be disordered. The major component of the disordered allyl ligand was refined to 0.718(8) and that of the disordered counteranion to 0.717(6). One void, which probably contains very disordered solvent molecules, was found at (−0.169, 0.748, 0.606). The contribution of these solvent molecules was taken out for the last stage of the refinement using the program SQUEEZE.<sup>40</sup> For both structures, the absolute configuration was established by the structure determination of a compound containing a chiral reference molecule of known absolute configuration and confirmed by

anomalous dispersion effects in diffraction measurements on the crystals. Geometry calculations were performed with the PLATON program.<sup>41</sup> Graphical illustrations were made using ORTEP-3 (2.02)<sup>42</sup> and Mercury 1.4.2 (Build 2).<sup>43</sup>

**Data for 4a:**  $\text{C}_{45}\text{H}_{36}\text{Cl}_2\text{F}_6\text{NO}_2\text{P}_3\text{Pd}$ ,  $M_w = 1006.96$ , colorless block,  $0.23 \times 0.12 \times 0.12$  mm<sup>3</sup>, monoclinic,  $P2_1$  (No. 4),  $a = 9.6088(2)$  Å,  $b = 41.1341(6)$  Å,  $c = 10.4629(2)$  Å,  $\beta = 91.581(1)^\circ$ ,  $V = 4133.88(13)$  Å<sup>3</sup>,  $Z = 4$ ,  $D_{\text{exptl}} = 1.618$  g cm<sup>−3</sup>,  $\mu = 0.76$  mm<sup>−1</sup>. 74 134 measured reflections, 18 886 unique reflections ( $R_{\text{int}} = 0.038$ ), 16 822 observed reflections using the criterion  $I > 2\sigma(I)$ . 1139 parameters refined with 217 restraints,  $R1/wR2$  ( $I > 2\sigma(I)$ ) 0.033/0.056,  $R1/wR2$  (all reflections) 0.043/0.058,  $S = 1.06$ , residual electron density between −0.47 and 0.58 e Å<sup>−3</sup>, Flack parameter<sup>44</sup> −0.018(10).

**Data for 5:**  $\text{C}_{38.5}\text{H}_{33}\text{ClF}_6\text{NO}_2\text{P}_3\text{Pd}$ ,  $M_w = 890.42^*$ , colorless block,  $0.19 \times 0.19 \times 0.16$  mm<sup>3</sup>, triclinic,  $P1$  (No. 1),  $a = 15.6617(4)$  Å,  $b = 15.8329(4)$  Å,  $c = 16.2065(5)$  Å,  $\alpha = 98.715(1)^\circ$ ,  $\beta = 92.600(1)^\circ$ ,  $\gamma = 90.599(2)^\circ$ ,  $V = 3967.63(19)$  Å<sup>3</sup>,  $Z = 4$ ,  $D_{\text{exptl}} = 1.491$  g cm<sup>−3\*</sup>,  $\mu = 0.72$  mm<sup>−1\*</sup>, 90 387 measured reflections, 36 340 unique reflections ( $R_{\text{int}} = 0.034$ ), 32 022 observed reflections using the criterion  $I > 2\sigma(I)$ . 1989 parameters refined with 421 restraints,  $R1/wR2$  ( $I > 2\sigma(I)$ ) 0.036/0.077,  $R1/wR2$  (all reflections) 0.046/0.080,  $S = 1.06$ , residual electron density between −0.68 and 0.87 e Å<sup>−3</sup>, Flack parameter<sup>44</sup> −0.016(8). SQUEEZE details: void of 319 Å<sup>3</sup> per unit cell filled with 55 electrons per unit cell. The asterisk indicates that the disordered solvent contribution was excluded.

**DFT Calculations.** The geometry optimization of complex **4b** was carried out with the Turbomole program<sup>45</sup> coupled to the PQS Baker optimizer.<sup>46</sup> Geometries were fully optimized as minima at the BP86<sup>47</sup> level using the SV(P) basis set on all atoms.<sup>48</sup>

**Acknowledgment.** This work was supported by NRSC-C and the European Union (RTN Revcat MRTN-CT-2006-035866). We thank J. A. J. Geenevasen for assistance with <sup>1</sup>H 2D NOESY experiments, J. W. H. Peeters for measuring high-resolution mass spectra and W. I. Dzik for DFT calculations. This work was also supported in part (A.L.S.) by the Council for the Chemical Sciences of The Netherlands Organization for Scientific Research (CW-NWO).

**Supporting Information Available:** Figures giving NMR spectra of complexes **4a,b** and **5** and CIF files giving crystallographic data for **4a** and **5**. This material is available free of charge via the Internet at <http://pubs.acs.org>.

OM801204A

(40) van der Sluis, P.; Spek, A. L. *Acta Crystallogr., Sect. A* **1990**, *46*, 194–201.

(41) Spek, A. L. *J. Appl. Crystallogr.* **2003**, *36*, 7–13.

(42) Farrugia, L. J. *J. Appl. Crystallogr.* **1997**, *30*, 565.

(43) Macrae, C. F.; Edgington, P. R.; McCabe, P.; Pidcock, E.; Shields, G. P.; Taylor, R.; Towler, M.; van de Streek, J. *J. Appl. Crystallogr.* **2006**, *39*, 453–457.

(44) Flack, H. D. *Acta Crystallogr., Sect. A* **1983**, *39*, 876–881.

(45) Treutler, O.; Ahlrichs, R. *J. Chem. Phys.* **1995**, *102*, 346–354.

(46) Baker, J. J. *Comput. Chem.* **1986**, *7*, 385–395.

(47) (a) Perdew, J. P. *Phys. Rev. B* **1986**, *33*, 8822–8824. (b) Becke, A. D. *Phys. Rev. A* **1988**, *38*, 3098–3100.

(48) Schäfer, A.; Horn, H.; Ahlrichs, R. *J. Chem. Phys.* **1992**, *97*, 2571–2577.

(34) COLLECT; Nonius BV, Delft, The Netherlands, 1999.

(35) Schreurs, A. M. M. PEAKREF; University of Utrecht, Utrecht, The Netherlands, 2005.

(36) Duisenberg, A. J. M.; Kroon-Batenburg, L. M. J.; Schreurs, A. M. M. *J. Appl. Crystallogr.* **2003**, *36*, 220–229.

(37) Beurskens, P. T.; Beurskens, G.; de Gelder, R.; Garcia-Granda, S.; Gould, R. O.; Smits, J. M. M. The DIRDIF2008 Program System; Crystallography Laboratory, University of Nijmegen, Nijmegen, The Netherlands, 2008.

(38) Sheldrick, G. M. *Acta Crystallogr., Sect. A* **2008**, *64*, 112–122.

(39) Sheldrick, G. M. SADABS 2006/1; University of Göttingen, Göttingen, Germany, 2006.